Collider signals and neutralino dark matter detection in relic-density-consistent models without universality

Howard Baer,[a] **Azar Mustafayev,**[b] **Eun-Kyung Park**[c] **and Xerxes Tata**[d]

[a]*Department of Physics, Florida State University, Tallahassee, FL 32306, U.S.A.*

[b]*Department of Physics and Astronomy, University of Kansas,*
Lawrence, KS 66045, U.S.A.

[c]*Physikalisches Institut, Universität Bonn, Nussallee 12, D53115 Bonn, Germany*

[d]*Department of Physics and Astronomy, University of Hawaii,*
Honolulu, HI 96822, U.S.A.

E-mail: baer@hep.fsu.edu, amustaf@ku.edu, epark@th.physik.uni-bonn.de,
tata@phys.hawaii.edu

ABSTRACT: We present brief synopses of supersymmetric models where either the neutralino composition or its mass is adjusted so that thermal relic neutralinos from the Big Bang saturate the measured abundance of cold dark matter in the universe. We first review minimal supergravity (mSUGRA), and then examine its various one-parameter extensions where we relax the assumed universality of the soft supersymmetry breaking parameters. Our goal is to correlate relic-density-allowed parameter choices with expected phenomena in direct, indirect and collider dark matter search experiments. For every non-universal model, we first provide plots to facilitate the selection of "dark-matter allowed" parameter space points, and then present salient features of each model with respect to searches at Tevatron, LHC and ILC and also direct and indirect dark matter searches. We present benchmark scenarios that allow one to compare and contrast the non-universal models with one another and with the paradigm mSUGRA framework. We show that many implications about sparticle properties and collider signals drawn from the analysis of the relic density constraint within mSUGRA do not carry over to simple one-parameter extensions of the mSUGRA framework. We find that in many relic-density-consistent models, there is one (or more) detectable edge in the invariant mass distribution of same-flavour, opposite sign dileptons in SUSY cascade decay events at the LHC. Finally, we scan the parameter space of these various models, requiring consistency with the LEP2 constraint on the chargino mass, and with the observed relic density, and examine prospects for direct and indirect dark matter detection. We find that in a large number of cases the mechanism that causes the early universe neutralino annihilation rate to be large (so as to produce the measured relic density) also enhances the direct detection rate, and often also the rates for indirect detection of neutralino dark matter.

KEYWORDS: Supersymmetry Phenomenology, Cosmology of Theories beyond the SM, Supersymmetric Standard Model.

Contents

1. Introduction and framework

An abundance of evidence arising from a variety of cosmological measurements shows that most of the matter in the Universe is not baryonic, but rather composed of massive neutral stable (or at least extremely long-lived), weakly (or super-weakly) interacting particles. Since none of the particles of the Standard Model (SM) have these properties, the existence of this so-called dark matter (DM) in the universe provides unequivocal evidence for physics beyond the SM.

Cosmological measurements severely constrain the abundance of DM: combining the results from the WMAP Collaboration with those from the Sloan Digital Sky Survey gives [1]

$$\Omega_{\rm DM}h^2 = 0.111^{+0.011}_{-0.015} \ \ (2\sigma) \,, \tag{1.1}$$

where $\Omega = \rho/\rho_c$ with ρ_c the closure density of the Universe, and h is the scaled Hubble parameter, $h = 0.73 \pm 0.04$. While the mass density of DM is rather precisely known, the identity of the DM particle remains a mystery. One class of candidates — thermally produced weakly interacting massive particles (WIMPS) — are especially appealing in that they naturally occur in a variety of well-motivated models, and further, because their relic density today (which can be reliably computed) is found to automatically have about the observed magnitude, provided the WIMP mass is of order the weak scale: $m_{\mathrm{WIMP}} \sim 100\,\mathrm{GeV}$. Of course, we should always bear in mind that, like visible matter, DM may consist of several components, so that, in standard Big Bang cosmology, (1.1) really implies an upper bound on the density of any single component.

Softly broken supersymmetry (SUSY), with a SUSY breaking scale below 1-2 TeV, is highly motivated for a variety of theoretical as well as experimental reasons [2, 3]. SUSY models with conserved R-parity include a stable, massive weakly interacting particle — the lightest neutralino $\widetilde{Z}_1$ in many models — which is perhaps the prototypical thermal WIMP [4]. In any supersymmetric model with a stable neutralino, the neutralino relic abundance can be reliably calculated as a function of model parameter space [5]. The result depends inversely on the thermally averaged neutralino-neutralino annihilation and co-annihilation cross sections, integrated over time from freeze-out to the present day. Once the parameters of the model under study are known to match the measured relic abundance (1.1) [6], then these select parameter space regions can be checked for phenomenological constraints from low energy measurements and from non-observation of new physics signals in the LEP and Fermilab Tevatron data. Implications for the on-going Tevatron run as well as for experiments soon-to-begin at the CERN LHC, and possibly at a TeV linear electron-positron collider in the future can be examined. Likewise, predictions can be made for rates of direct detection of relic neutralinos via scattering on nuclear targets, or rates for indirect neutralino detection, either via ν_μ signals from neutralino annihilation in the solar core, or via galactic halo annihilations which can give rise to gamma ray or anti-matter ($\bar{p}$, e^+ or $\bar{D}$) signals.

Most analyses of neutralino dark matter have been carried out in the context of the minimal supergravity model — mSUGRA [7] where SUSY breaking, which occurs in a hidden sector, is communicated to the observable sector via gravitational interactions. The universality of soft SUSY breaking (SSB) parameters, renormalized at a scale $Q \simeq M_{\mathrm{GUT}} - M_P$ is the hallmark of this framework. Specifically, one assumes that the mediation mechanism induces a common mass parameter m_0 for all MSSM scalars, a common gaugino mass $m_{1/2}$ for gauginos, a common trilinear SSB parameter A_0 together with a bilinear Higgs scalar mass b, in the effective MSSM Lagrangian, with parameters renormalized at $Q = M_{\mathrm{GUT}}$. It is also assumed that the dimensionful SSB parameters all have the magnitude of the weak scale. The large top quark Yukawa coupling drives the celebrated radiative electroweak symmetry breaking (REWSB) mechanism, and automatically leads to the $\mathrm{SU}(3)_C \times \mathrm{U}(1)_{\mathrm{EM}}$ symmetric vacuum over a significant portion (but not all) of the model parameter space. The GUT scale SSB parameter b can be traded for $\tan\beta$, the ratio of Higgs field vevs, while the magnitude (but not the sign) of the superpotential mass parameter μ is fixed by the observed value of M_Z. The mSUGRA model is thus completely

specified by the parameter set

$$m_0, \ m_{1/2}, \ A_0, \ \tan\beta, \ sign(\mu), \qquad\qquad (1.2)$$

along with the value of the top quark mass m_t. Except where explicitly mentioned, we fix $m_t = 171.4\,\text{GeV}$, in accord with recent top mass measurements at the Fermilab Tevatron [8].

Unless sparticles are very light ($\sim 100\,\text{GeV}$) the generic value of the relic density in mSUGRA (as well as in many other SUSY models) tends to be well in excess of the observed CDM relic density (1.1). As a result, only special regions of the mSUGRA parameter space where the annihilation rate for neutralinos is enhanced are compatible with the measured value of the relic density.[1] In early work on the mSUGRA model, the low m_0, low $m_{1/2}$ region (so-called "bulk region"), where sparticles are indeed very light, was favored [9, 13] in that neutralino annihilation into leptons via light $t-$channel slepton exchange occurred at large rates, leading to relic densities $\Omega_{\widetilde{Z}_1}h^2 \sim 0.3 - 1$. The rather lower measured abundance in (1.1), however, favors even lower values of m_0 and $m_{1/2}$, resulting in considerable tension with the negative search results from LEP2 for chargino and slepton pair production. Within the mSUGRA framework, the remaining relic-density-allowed regions consist of:

- The stau-co-annihilation region at low m_0 and low-to-moderate values of $m_{1/2}$ where $m_{\tilde{\tau}_1} \sim m_{\widetilde{Z}_1}$, so that neutralinos can co-annihilate with staus [10] in the early universe.

- The hyperbolic branch/focus point (HB/FP) region [11] at very large m_0 values where $|\mu|$ becomes small so that $\widetilde{Z}_1$ becomes a mixed bino-higgsino state. In this case, $\widetilde{Z}_1\widetilde{Z}_1$ annihilation to WW, ZZ and Zh via the $\widetilde{Z}_1$ higgsino component is enhanced in the early universe.

- The Higgs funnel region at large $\tan\beta \sim 50$ [12], where $2m_{\widetilde{Z}_1} \sim m_A$, so that neutralinos can annihilate at an enhanced rate through the (wide at large $\tan\beta$) A (or H) resonance. An h-resonance annihilation strip can also occur at low $m_{1/2}$, where $2m_{\widetilde{Z}_1} \simeq m_h$ [13].

- The top squark co-annihilation region at large negative A_0 values where $m_{\widetilde{Z}_1} \sim m_{\tilde{t}_1}$ so that $\widetilde{Z}_1$ can co-annihilate with $\tilde{t}_1$ particles [14].

The regions of mSUGRA parameter space leading to a neutralino relic density in agreement with (1.1) are all near the edges of theoretically (or in the case of h resonance annihilation, experimentally) allowed parameter space, which can lead one to question whether the mSUGRA model might be *disfavored* by the measured neutralino relic abundance. In this vein, many authors have examined SUGRA-type models but with *non-universal* soft term boundary conditions at $Q \sim M_{\text{GUT}}$. It is appropriate to note here that unfettered non-universality of soft terms generically leads to the occurrence of flavor changing processes

---

[1]In our analysis, we are assuming that thermally produced neutralinos in the standard Big Bang cosmology make up the DM. While it is possible to get around these assumptions, we feel that an examination of the conceptually simplest scenario that does not invoke additional hypotheses warrants special attention.

at levels far beyond experimental limits [15]. With this in mind, we work in a simplified parameter space wherein there exists degeneracy or near degeneracy of first and second generation scalar masses, leading to a suppression of FCNC processes via the super-GIM mechanism. At the same time, in order to maintain the obvious success of gauge coupling unification, we must assume that the correct effective theory between the weak and GUT scales is the MSSM, or the MSSM augmented by gauge singlets, or the MSSM together with additional matter in complete multiplets of SU(5).

With these considerations in mind, we will assume that:

1. In the interests of minimality, while maintaining the successful predictions of gauge coupling unification, that the MSSM is the correct effective field theory between M_{weak} and M_{GUT}.

2. The REWSB mechanism leads to an $\text{SU}(3)_C \times \text{U}(1)_{\text{EM}}$ symmetric ground state; i.e. electric charge and color gauge symmetries are not spontaneously broken.

3. CP violating phases in the SSB parameters are suppressed so that supersymmetric contributions to CP violating processes are sufficiently small [16].

4. There is a near-degeneracy of SSB of the first and second generation sfermions so that SUSY contributions to flavor-violating processes is automatically suppressed. We do allow some non-degeneracy between third generation scalars and first or second generation scalars.

5. R-parity is conserved so that the lightest supersymmetric particle (LSP) is stable.

6. The gravitino — which in models with gravity-mediated SUSY breaking naturally has a mass of order M_{weak} — is not the LSP, which we take instead to be the lightest neutralino. For a discussion of the possibility that a gravitino LSP is the DM, see ref. [17].

In the spirit of our earlier discussion we need to relax the theoretically least well-motivated universality assumption that underlies the mSUGRA framework in a controlled manner (to avoid large flavor-violating couplings) and explore non-minimal SUGRA models with an expanded parameter space. We could, for instance, consider a non-minimal model where we independently vary,

$$M_1, \ M_2, \ M_3 \qquad \text{(gaugino masses)}, \tag{1.3}$$
$$m_0(1,2) \qquad \text{(common first/second generation SSB matter scalar masses)}, \tag{1.4}$$
$$m_0(3) \qquad \text{(common third generation SSB matter scalar masses)}, \tag{1.5}$$
$$m_{H_u}^2, \ m_{H_d}^2 \qquad \text{(non − universal SSB Higgs mass parameter)}, \tag{1.6}$$
$$A_t, \ A_b, \ A_\tau \qquad \text{(non − universal third gen. } A \text{ terms)}, \tag{1.7}$$
$$\tan\beta, \tag{1.8}$$
$$sign(\mu). \tag{1.9}$$

A different but equally reasonable option may be to require common masses for matter scalars with the same gauge quantum numbers but allow intra-generation splittings. In this case, we would have common mass parameters m_Q^2, m_U^2, m_D^2, m_L^2 and m_E^2 at $Q = M_{\rm GUT}$. In the extreme case, the matter scalar masses can be further broken down into specific soft term masses $m_{Q_i}^2$, $m_{U_i}^2$, $m_{D_i}^2$, $m_{L_i}^2$, $m_{E_i}^2$ where $i = 1-3$ for each generation. These options have been explored elsewhere [18, 19], and will not be discussed further in this paper.

One way to proceed is to perform scans over the much larger non-minimal SUGRA parameter space and search for solutions which satisfy dark matter (and also other) constraints. While this approach has the virtue of being unbiased in the scanning, it is practically difficult to implement. Moreover, when a large number of free parameters are varied simultaneously, it is frequently difficult to draw insights into the associated dark matter and collider phenomenology that follow. Instead, many groups [20 − 26, 85] have examined the impact of relaxing the underlying universality of the mSUGRA model in a controlled way, by allowing non-universal parameters only in one sector of parameter space at a time. For instance, we may consider the mSUGRA parameter space augmented to accommodate non-universal gaugino mass parameters [27] as in (1.3), or instead extended to allow Higgs boson SSB mass parameters to be different from matter scalar mass parameters as in (1.6), but not both. Other directions in the parameter space of the non-minimal SUGRA models can be similarly explored. These extensions generally require augmenting the mSUGRA space by just one (sometimes, two) additional parameter that is adjusted to yield agreement with the observed DM relic density. The phenomenological implications of the extended model as a function of the remaining mSUGRA parameters can be readily examined, and directly compared with the paradigm mSUGRA framework. This approach has led to new insights and to exciting new possibilities for collider and dark matter phenomenology that can be expected in models with non-universal soft SUSY breaking terms.

Examination of these simple one-parameter extensions of mSUGRA leads to another important pay-off. Since, as discussed above, analyses of the relic density constraint in mSUGRA force parameters to be in the bulk region, the stop or stau co-annihilation region, the Higgs funnel region or the HB/FP region of parameter space, many groups have inferred that at least one of the following must hold:

1. Sfermions have masses $\sim 100\,{\rm GeV}$ (bulk region), and so must be accessible at the LHC.

2. There is at least one charged sparticle close in mass to the LSP, so that this should be accessible at the LHC, unless the LSP is so heavy that the hard-won gauge hierarchy is again destabilized (co-annihilation).

3. The additional Higgs scalars of the MSSM are relatively light with $m_A \sim 2m_{\widetilde{Z}_1}$ so that these can be searched for at the LHC, which requires large values of $\tan\beta$ where sparticles preferentially decay to third generation quarks and leptons (Higgs resonance region).

4. The lightest neutralino has a significant higgsino component, which is possible only

if m_0 is so large that squarks and sleptons are essentially inaccessible at the LHC (HB/FP region).

It is imperative, of course, to check the robustness of these "predictions" to minor variations of the assumptions underlying mSUGRA before drawing broad conclusions about what the relic density determination implies for experiments at the LHC, as well as for direct and indirect detection of DM. Our study of the various extensions of mSUGRA naturally permits this.

In this paper, we have two broad goals. The first, in section 2, is to present an overview of a number of different models, wherein by tuning one additional parameter beyond those of the mSUGRA model we can match the predicted neutralino relic abundance with (1.1). Models wherein the *composition* of the neutralino is adjusted to obtain the measured relic abundance are referred to as "well-tempered neutralino" models (WTN) [28]. We also examine several models wherein neutralino or other sparticle *masses* are adjusted to obtain the correct relic abundance of dark matter.

In each case, we present *i.*) motivation, *ii.*) the parameter space, and selected parameter values that allow the reader to generate spectra and collider events for the particular model. We also comment on the salient features of *iii.*) collider and *iv.*) dark matter search phenomenology associated with each particular model. For our analysis, we adopt the SUSY spectrum generator Isasugra, a part of the event generator ISAJET 7.76 [29]. For any given parameter set satisfying the DM relic density constraint (1.1), the sparticle mass spectrum and associated neutralino relic density and direct and indirect detection rates may be calculated, and associated collider events may be generated for the Tevatron, LHC or ILC colliders. To facilitate comparison with the paradigm mSUGRA case, we first present an updated overview of allowed regions within mSUGRA. In section 3, we present some benchmark cases where the spectra and some results from these various models are explicitly compared with the corresponding situation in the mSUGRA case.

Our second goal, presented in section 4, is to extract several general results from scans over the models examined in section 2, to gain an idea of some of the features relevant to collider and dark matter searches that might be shared by many of these models. For instance, it has already been pointed out that the subset of these models which resolve the dark matter relic density problem via mixed gaugino/higgsino dark matter (i.e. models with a WTN) collectively have neutralino-nucleon direct detection scattering rates that asymptote around $\sim 10^{-8}$ pb [30], putting them within reach of direct dark matter search experiments currently being mounted, such as SuperCDMS, LUX, Xenon-100, WARP and mini-CLEAN. Also, models with non-universality where the composition is tempered to yield the observed relic density, or where agreement with (1.1) is obtained via bino-wino co-annihilation, tend to have a neutralino mass gap $m_{\widetilde{Z}_2} - m_{\widetilde{Z}_1}$ smaller than M_Z, so that three body decay modes dominate the $\widetilde{Z}_2$ branching fraction. Unless the leptonic branching fraction of the neutralino happens to be strongly suppressed [31], this then yields an observable mass edge in the dilepton mass spectrum at $m(\ell^+\ell^-) = m_{\widetilde{Z}_2} - m_{\widetilde{Z}_1}$, which serves as a good starting point for sparticle mass reconstruction in gluino and squark cascade decay events at the CERN LHC [32].

We conclude in section 5 with a summary of our results together with some general comments.

2. Brief synopses of SUSY models with neutralino dark matter

2.1 The mSUGRA model

We begin by presenting updated results on the allowed parameter space of the minimal supergravity model. The mSUGRA model is completely specified by the parameter set (1.2). To calculate the sparticle mass spectrum, we use ISAJET 7.76 [29]. The relic density is evaluated via the IsaReD program [10], which is part of the IsaTools package. IsaReD evaluates all $2 \rightarrow 2$ tree-level neutralino annihilation and co-annihilation processes and implements relativistic thermal averaging in the relic density calculation.

For our first results, we show in figure 1 the m_0 *vs.* $m_{1/2}$ plane for parameters $A_0 = 0$, $\tan\beta = 10$ and $\mu > 0$ with *a*) $m_t = 170\,\text{GeV}$, *b*) $m_t = 171.4\,\text{GeV}$ and *c*) $m_t = 175\,\text{GeV}$. The red-shaded regions on the left are excluded because $\tilde{\tau}_1$ becomes the LSP, while the red-shaded regions on the lower right are excluded due to a failure to meet the EWSB minimization conditions. The blue-shaded region is theoretically allowed, but is experimentally excluded by LEP2 searches for chargino pair production where we require $m_{\widetilde{W}_1} > 103.5\,\text{GeV}$ [33]. The negative results of Higgs boson searches at LEP2 [34] require that the SM Higgs boson is heavier than $114.1\,\text{GeV}$. This limit can be translated to a lower limit on the MSSM Higgs boson mass. While $h \simeq H_{\text{SM}}$ if m_A is large, in general the bound on m_h depends on MSSM parameters, including CP violating phases that we have ignored in our analysis. The evaluation of m_h is also uncertain to about $\sim 3\,\text{GeV}$ due to missing two-loop corrections [35]. For these reasons, we do not include any bound on m_h in the LEP2-excluded blue region, but only show the boundary of the region $m_h \leq 110\,\text{GeV}$ by the magenta contour (lower-left) in the figure. The green regions have a neutralino relic density in accord with (1.1): $0.094 < \Omega_{\widetilde{Z}_1}h^2 < 0.129$. In the yellow regions, however, $\Omega_{\widetilde{Z}_1}h^2 < 0.094$, so that an additional component of dark matter particles is necessary to saturate the observed DM relic density. The remaining unshaded regions all have $\Omega_{\widetilde{Z}_1}h^2 > 0.129$, i.e., they give rise to *too much* dark matter: thus, these are excluded in standard Big Bang cosmology. We also show contours of gluino and first generation squark masses; these contours hardly change under variation of A_0, $\tan\beta$ and $sign(\mu)$, except at the level of one loop corrections and D-term contributions to their masses.

The hard-to-see green/yellow region adjacent to the $\tilde{\tau}_1$-$\widetilde{Z}_1$ region shows up as a very narrow sliver where the $\tilde{\tau}_1 - \widetilde{Z}_1$ mass gap is small enough so that stau co-annihilation occurs at a large rate. This region in fact appears jagged only due to the resolution of our parameter space scans. One can also see the HB/FP region — where $|\mu|$ becomes comparable to the SU(2) and U(1) gaugino masses and the $\widetilde{Z}_1$ becomes mixed higgsino dark matter — adjacent to the EWSB forbidden region as the wider green/yellow shaded region at large m_0, starting at $m_{1/2} \sim 300\,\text{GeV}$, which corresponds to the turn-on point for $\widetilde{Z}_1\widetilde{Z}_1 \rightarrow W^+W^-$; for lower $m_{1/2}$ values, this annihilation channel is closed, and the neutralino annihilation rate (via Z^* exchange) generally becomes too small to bring the relic density into accord with (1.1).
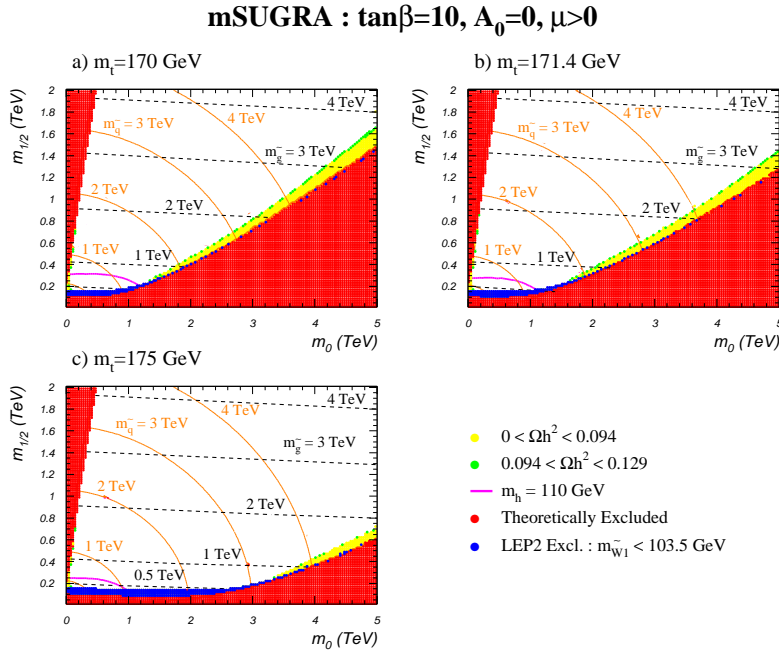
mSUGRA : tanβ=10, A₀=0, μ>0

Figure 1: A plot of the m_0 $vs.$ $m_{1/2}$ plane in mSUGRA for $A_0 = 0$, $\tan\beta = 10$ with $\mu > 0$ and a) $m_t = 170\,\text{GeV}$, b) $m_t = 171.4\,\text{GeV}$ and c) $m_t = 175\,\text{GeV}$. The red-shaded regions are excluded because electroweak symmetry is not correctly broken, or because the LSP is charged. Blue regions are excluded by direct SUSY searches at LEP2. Yellow and green shaded regions are WMAP-allowed, while white regions are excluded owing to $\Omega_{\widetilde{Z}_1} h^2 > 0.129$. Also shown are gluino and first generation squark mass contours, as well as a magenta contour below which $m_h \leq 110\,\text{GeV}$.

While these three frames for the different m_t values are qualitatively similar, the main effect of m_t variation shows up in the location of the EWSB excluded region, and hence the location of the adjacent HB/FP region: on the low side of the allowed m_t range, the HB/FP region moves to m_0 values as low as 1.5 TeV, while at the high end of this range, the HB/FP region only starts when $m_0 \gtrsim 3\,\text{TeV}$ [36].

In figure 2, we show the m_0 $vs.$ $m_{1/2}$ plane for $A_0 = 0$, $\mu > 0$, $m_t = 171.4\,\text{GeV}$, and for six different values of $\tan\beta$. We see that for $\tan\beta = 10$ only the stau co-annihilation and HB/FP regions are DM-allowed. As $\tan\beta$ is increased, more and more parameter space comes into accord with (1.1). Already for $\tan\beta = 45$, a small DM-allowed region appears at low m_0 and low $m_{1/2}$. The reason is that as $\tan\beta$ grows, the b and τ Yukawa couplings become large, causing m_A to drop. Thus, $\widetilde{Z}_1\widetilde{Z}_1 \to A^* \to b\bar{b}$, $\tau^+\tau^-$ becomes more and more important, even if one is not "right on the A resonance" [12]. The low m_0, $m_{1/2}$ allowed region grows even more at $\tan\beta = 50$. At $\tan\beta = 52$, the A- funnel annihilation region has just come into view on the left edge of parameter space. By $\tan\beta = 54$, the A-funnel is extremely broad due to the large A width: $\Gamma_A \sim 10\,\text{GeV}$ (50 GeV) for low (high) $m_{1/2}$. We notice at $\tan\beta = 55$, a small red-shaded wedge invades the plot at low m_0 and $m_{1/2}$. In this region, the value of $m_h^2 < 0$, signaling collapse of EWSB. For somewhat higher $\tan\beta$ values, the entire parameter space collapses.
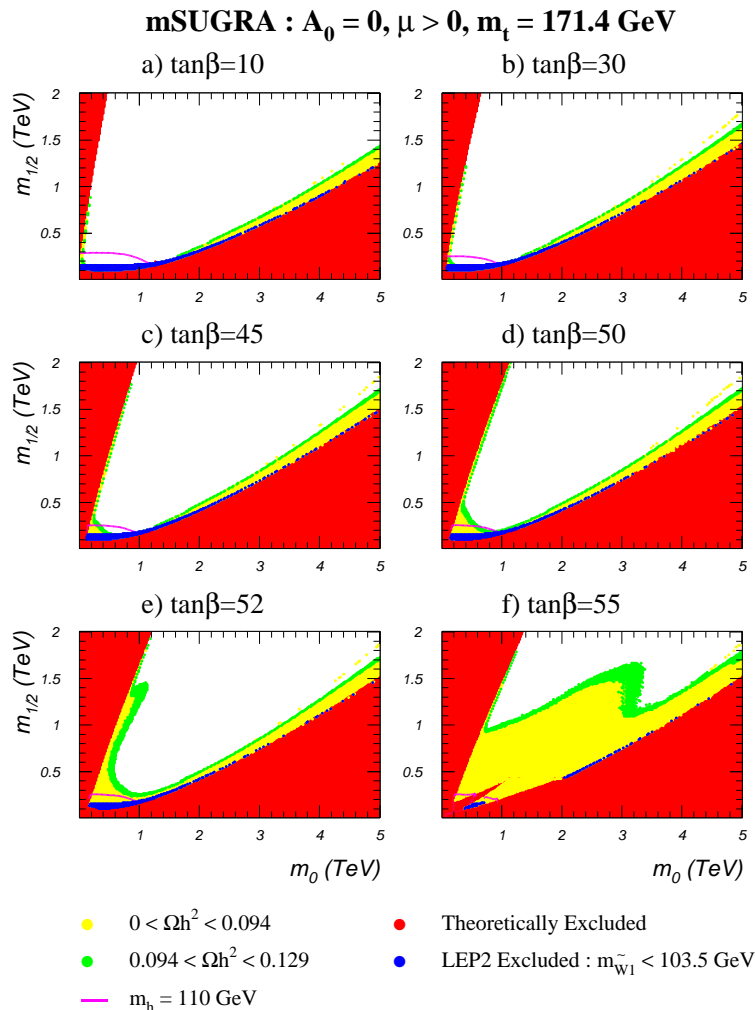
mSUGRA : $A_0 = 0$, $\mu > 0$, $m_t = 171.4$ GeV

a) tanβ=10 b) tanβ=30 c) tanβ=45 d) tanβ=50 e) tanβ=52 f) tanβ=55

$m_{1/2}$ (TeV) m_0 (TeV)

- $0 < \Omega h^2 < 0.094$ (yellow)
- $0.094 < \Omega h^2 < 0.129$ (green)
- $m_h = 110$ GeV (magenta)
- Theoretically Excluded (red)
- LEP2 Excluded : $m_{\widetilde{W}_1} < 103.5$ GeV (blue)

Figure 2: A plot of the m_0 *vs.* $m_{1/2}$ plane in mSUGRA for $A_0 = 0$ and various values of $\tan\beta$, with $\mu > 0$ and $m_t = 171.4$ GeV. The red-shaded regions are excluded because electroweak symmetry is not correctly broken, or because the LSP is charged. Blue regions are excluded by direct SUSY searches at LEP2. Yellow and green shaded regions are WMAP-allowed, while white regions are excluded owing to $\Omega_{\widetilde{Z}_1} h^2 > 0.129$. Below the magenta contour in each frame, $m_h < 110$ GeV.

In figure 3, we show the same m_0 *vs.* $m_{1/2}$ planes as in figure 2 for multiple $\tan\beta$ values, but this time for $\mu < 0$. This sign of μ is disfavored by the Muon $g-2$ Collaboration measurements of anomalous magnetic moment $(g-2)_\mu$ at low m_0 and low $m_{1/2}$ [37]. At high m_0 and $m_{1/2}$ values, sparticle contributions to the muon QED vertex decouple, and the deviation from SM predictions is tiny for either sign of μ. We also see that the A-funnel arises in the m_0 *vs.* $m_{1/2}$ plane at somewhat lower $\tan\beta$ values. The A-funnel is actually narrower than in the $\mu > 0$ case, in part because the A width is narrower. We also see a bulge of incorrect EWSB beginning already at $\tan\beta = 45$, and growing so as to engulf nearly all parameter space by $\tan\beta = 55$.
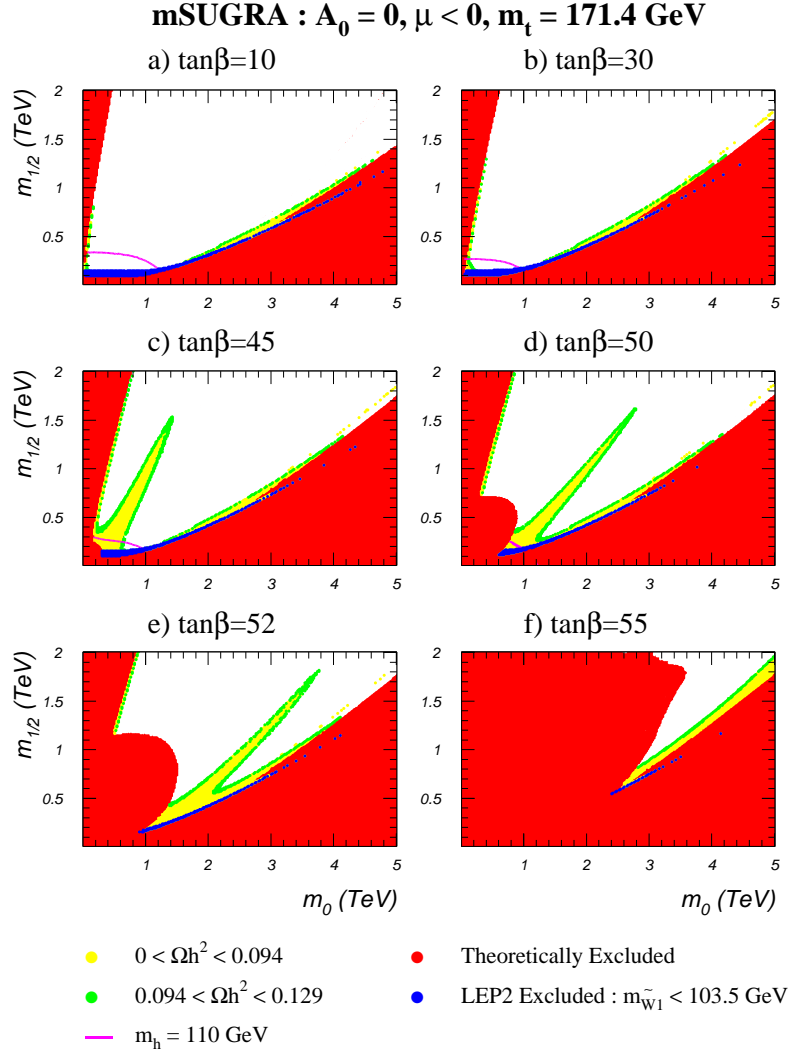
mSUGRA : A$_0$ = 0, μ < 0, m$_t$ = 171.4 GeV

a) tanβ=10 b) tanβ=30

c) tanβ=45 d) tanβ=50

e) tanβ=52 f) tanβ=55

$m_{1/2}$ (TeV)

m_0 (TeV)

- (yellow) $0 < \Omega h^2 < 0.094$
- (green) $0.094 < \Omega h^2 < 0.129$
- (magenta) $m_h = 110$ GeV
- (red) Theoretically Excluded
- (blue) LEP2 Excluded : $m_{\widetilde{W}_1} < 103.5$ GeV

Figure 3: A plot of the m_0 $vs.$ $m_{1/2}$ plane in mSUGRA for $A_0 = 0$ and various values of $\tan\beta$, with $\mu < 0$ and $m_t = 171.4$ GeV. The red-shaded regions are excluded by lack of correct EWSB or by the presence of a charged LSP. Blue regions are excluded by direct SUSY searches at LEP2. Yellow and green shaded regions are WMAP-allowed, while white regions are excluded owing to $\Omega_{\widetilde{Z}_1} h^2 > 0.129$. Below the magenta contour in frames a)-d) $m_h < 110$ GeV , while $m_h > 110$ GeV all over the LEP2 allowed region in frames e) and f).

We see from figure 3 that the Higgs funnel moves to larger values of m_0 as we increase $\tan\beta$. To understand this, we take a point $(m_0, m_{1/2})$ in the funnel where $m_A \simeq 2m_{\widetilde{Z}_1}$, and examine what would happen if we increase $\tan\beta$ keeping the other parameters fixed. We first remark that because $\widetilde{Z}_1$ is essentially a bino, $m_{\widetilde{Z}_1} \simeq M_1$ remains essentially unaltered. The behaviour of $m_A^2 \sim m_{H_d}^2 - m_{H_u}^2$ is governed by how the evolution of the Higgs scalar SSB parameters is altered by the increase in $\tan\beta$. In the case where the evolution of $m_{H_u}^2$

JHEP05(2008)058

$(m^2_{H_d})$ is dominated by the term $3f^2_t X_t$ $(3f^2_b X_b)^2$ in their one-loop RGE [2],[3] we see that — since f_b increases with $\tan\beta$ while f_t is left essentially unaltered — the weak scale values of $m^2_{H_d}$ and $m^2_{H_u}$ move closer to each other so that m^2_A is reduced. As a result, for a larger $\tan\beta$ value the point will move out of the A-funnel region (modulo effects of the width of A) because m_A becomes smaller than $2m_{\widetilde{Z}_1}$. To return to the A-funnel region, we must have a larger value of X_t to also move $m^2_{H_u}$ to more negative values compensating for the reduction of m_A with the increase in $\tan\beta$. For a fixed value of A_0, this means increasing m_0, explaining why the Higgs funnel moves to the right as we increase $\tan\beta$ in figure 3. A qualitatively similar behaviour can also be seen in figure 2, but just in the last two frames since for $\mu > 0$ the Higgs funnel does not appear for the other choices of $\tan\beta$.

A similar analysis can also help us to understand how the location of the Higgs funnel in the $m_0 - m_{1/2}$ plane depends on the choice of m_t. For larger values of m_t, and thus of f_t, $m^2_{H_u}$ evolves to more negative values while the evolution of $m^2_{H_d}$ remains essentially unaltered. Thus we move out of the A-funnel because now m_A becomes *larger* than $2m_{\widetilde{Z}_1}$, and to return to the A-funnel we must now reduce m_0, so that the A-funnel (if it occurs) moves to smaller values of m_0 as m_t is increased. Although we do not show figures here, we have verified that this is indeed the case for representative slices of the $m_0 - m_{1/2}$ plane.

Up to now in all our plots we have assumed $A_0 = 0$. By changing the A_0 parameter, one is altering the intra-generation mixing between third generation sfermions, especially the top squarks. This mixing also reduces $m_{\tilde{t}_1}$. In figure 4, we show the m_0 $vs.$ $m_{1/2}$ plane for $\tan\beta = 10$, $A_0 = -2\,\mathrm{TeV}$ and $\mu > 0$. In this case, a forbidden region appears at low m_0 and $m_{1/2}$, where the $\tilde{t}_1$ becomes the LSP. Along the edge of this region, a yellow/green band appears: the stop co-annihilation region, where the $\tilde{t}_1 - \widetilde{Z}_1$ mass gap is positive but quite small, so that $\widetilde{Z}_1$ can co-annihilate against $\tilde{t}_1$ in the early universe, thus giving a relic density matching (1.1). We also see an h-annihilation strip at low $m_{1/2}$ and $m_0 \sim 2.75\,\mathrm{TeV}$, where $2m_{\widetilde{Z}_1} \simeq m_h$ and neutralino annihilations into SM fermions are resonantly enhanced.

2.2 Models with scalar mass non-universality

2.2.1 Generational non-universality: normal scalar mass hierarchy

Motivation: the normal scalar mass hierarchy model (NMH) examines the effect of generational non-universality in the SSB sfermion mass parameters [38, 20, 39]. While constraints from $K - \bar{K}$ mass difference restrict first and second generation scalar masses to be nearly universal, the constraints arising from $B - \bar{B}$ mixing are much less strict, and some non-universality of third generation matter scalars compared to first/second generation matter scalars can be allowed. In fact, it can be argued that the data actually favor such a case: we know that the measured value of $BF(b \rightarrow s\gamma)$ is in rather close accord with SM predictions, suggesting that the third generation sparticles that enter the $b \rightarrow s\gamma$ loop diagrams are rather heavy– of order the TeV scale. Meanwhile, the $2 - 3\sigma$ discrepancy of

---

[2]Here, $X_t = m^2_{Q_3} + m^2_{\tilde{t}_R} + m^2_{H_u} + A^2_t$ and $X_b = m^2_{Q_3} + m^2_{\tilde{b}_R} + m^2_{H_d} + A^2_b$.

[3]This will be the case as long as squark masses and A-parameters are not simultaneously very small, since for the large values of $\tan\beta$ where the Higgs funnel occurs, the Yukawa couplings are typically larger than the electroweak gauge couplings.

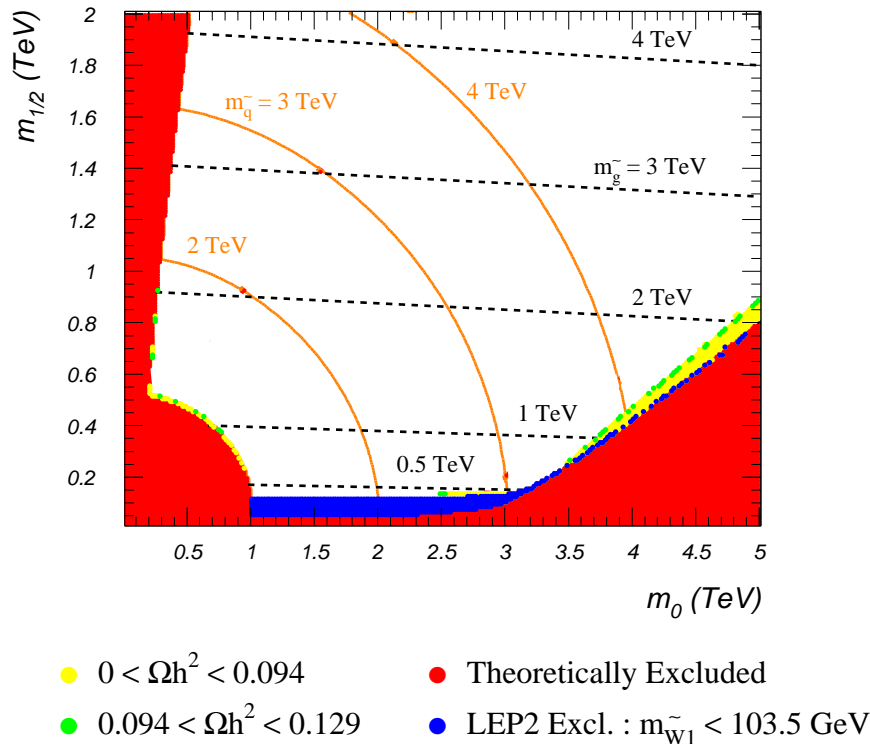**mSUGRA : tanβ=10, A₀=-2 TeV, μ>0, mₜ=171.4 GeV**

Figure 4: A plot of the m_0 vs. $m_{1/2}$ plane in mSUGRA for $A_0 = -2\,\text{TeV}$, $\tan\beta = 10$ with $\mu > 0$ and $m_t = 171.4\,\text{GeV}$. The red-shaded regions are excluded by lack of correct EWSB or by presence of a charged LSP. Blue regions are excluded by direct SUSY searches at LEP2. Yellow and green shaded regions are WMAP-allowed, while white regions are excluded owing to $\Omega_{\widetilde{Z}_1} h^2 > 0.129$. This plot includes a top-squark co-annihilation region adjacent to the excluded bulge at low m_0 and low $m_{1/2}$ as well as an $h-$annihilation strip at low $m_{1/2}$ and $m_0 \sim 2.75\,\text{TeV}$. Throughout the LEP2 allowed region, $m_h > 114\,\text{GeV}$.

the measured $(g-2)_\mu$ against the SM prediction seems to favor rather light, sub-TeV scale smuon and muon sneutrino masses. A normal scalar mass hierarchy at the GUT scale with $m_0(1,2) \ll m_0(3)$ can reconcile the apparent tension between $BF(b \to s\gamma)$ and $(g-2)_\mu$ in SUSY models, and give a relic density in accord with (1.1).

Parameter space: the parameter space of the NMH model is given by

$$m_0(1,2), \ m_0, \ m_{1/2}, \ A_0, \ \tan\beta, \ sign(\mu) \tag{2.1}$$

where $m_0(1,2)$ is the common GUT scale matter scalar mass parameter for first/second generation scalars at M_{GUT}, while $m_0(3) = m_{H_u} = m_{H_d} \equiv m_0$ defines the remaining

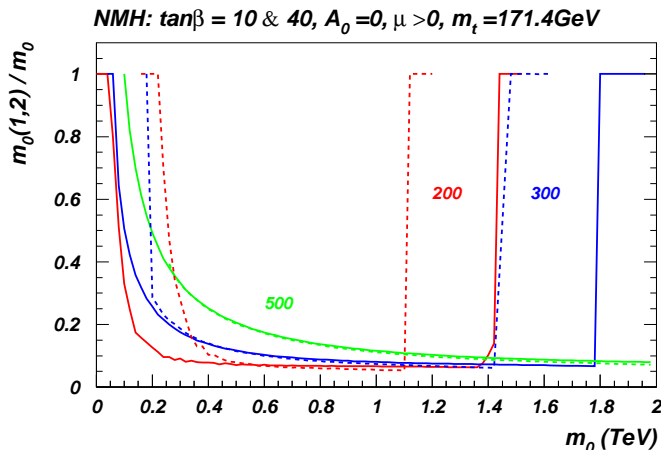**NMH: tan β = 10 & 40, A₀ =0, μ >0, mₜ =171.4GeV**

Figure 5: The value of $m_0(1,2)/m_0$ needed to bring various mSUGRA points into accord with the measured relic density versus m_0, for $A_0 = 0$, $\mu > 0$, and $\tan\beta = 10$ (solid lines) and 40 (dashed lines) in the NMH scenario. The three sets of curves correspond to $m_{1/2}$ values of 200, 300 and 500 GeV.

scalar mass parameter, again at $Q = M_{\rm GUT}$. The Higgs scalar masses are taken here to be degenerate with $m_0(3)$, but could be independent as well.

If we begin with a generic point in mSUGRA parameter space where $\Omega_{\widetilde{Z}_1} h^2 \gg 0.129$, and then dial $m_0(1,2)$ to successively lower values, the first/second generation slepton masses fall until they are low enough that bulk neutralino annihilation via light sleptons and/or neutralino-slepton co-annihilation acts to reduce the relic density to WMAP-allowed levels. As a result of lowering $m_0(1,2)$, sleptons tend to be quite light. However, first/second generation squark masses are typically pulled up via RG running into the several hundred GeV to a TeV range.

In figure 5, we show the ratio $m_0(1,2)/m_0$ needed to reduce the relic density to the WMAP allowed value versus m_0. We show results for three choices of $m_{1/2}$: 200, 300 and 500 GeV. Solid curves are for $\tan\beta = 10$ while dashed curves are for $\tan\beta = 40$. We fix $A_0 = 0$ and take $\mu > 0$. At quite low m_0, we are already in the stau co-annihilation region (bulk region for $m_{1/2} = 200$ GeV), so little or no reduction of $m_0(1,2)$ is needed. The curves terminate at the left because for still smaller values of m_0, we hit the stau LSP region. As m_0 increases, a large reduction is needed to match the measured relic density, where ratios $m_0(1,2)/m_0 \sim 0.1$ are common. At very large m_0, no reduction in $m_0(1,2)/m_0$ is again necessary as we enter the HB/FP region.

Implications for collider searches: the very small first/second generation slepton masses in the NMH model imply that these will likely be directly accessible to LHC searches [40]. Even if this is not the case, branching ratios for chargino and neutralino decays to leptons via 2 or 3 body modes will be considerably enhanced, leading to SUSY cascade decay events at the LHC that are much richer in hard, isolated leptons than would be expected in the mSUGRA model. Meanwhile, selectron and smuon pair production — but not stau pair production — would likely be accessible to ILC searches.

Implications for DM searches: while neutralino annihilation in the early universe is enhanced via light slepton exchange or slepton co-annihilation, squarks remain relatively heavy, and the neutralino is largely bino-like. Thus, both direct and indirect DM search predictions will be qualitatively similar to those generated in the mSUGRA model with $m_0(3) \sim m_0$. For the case that we study in table 1 below, we have explicitly checked that even the indirect detection signals at IceCube and Pamela detectors remain small despite the reduced masses of first/second generation sneutrinos and charged sleptons.

2.2.2 Non-universal Higgs mass: one extra parameter case

Motivation: in supersymmetric grand unified theories based upon the gauge group SO(10), the matter superfields of a single generation are contained in a 16-dimensional spinor representation of SO(10), ψ_{16}, which includes, in addition, a SM gauge singlet right-handed neutrino superfield. The Higgs superfields can be most simply accommodated in the fundamental 10-dimensional representation ϕ_{10}. It is natural to expect that different multiplets would receive different soft masses at the GUT scale. Even if the soft masses for Higgs and matter scalars were common at some scale near M_P, RG running effects in the SO(10) theory would split the soft terms at M_{GUT} (see ref. [18] for explicit examples of soft term running in SO(10) SUSY GUTs).

Parameter space: in the non-universal Higgs model with one additional parameter (NUHM1) [21], the matter scalars receive a common squared mass parameter m_0^2 at $Q = M_{\mathrm{GUT}}$, while both SU(2) Higgs scalar doublets H_u and H_d acquire equal values for their SSB parameters, that are different from m_0^2. Note that $m_{H_u}^2 (= m_{H_d}^2)$ is just a parameter, not a physical mass squared, so its value can be either positive or negative (as can m_0^2 [41]). The parameter space is thus given by

$$m_0, \ \delta_\phi, \ m_{1/2}, \ A_0, \ \tan\beta, \ sign(\mu), \tag{2.2}$$

where $m_\phi = m_0(1 + \delta_\phi)$ and $m_{H_u}^2 = m_{H_d}^2 \equiv sign(m_\phi) \cdot |m_\phi|^2$ at the GUT scale.

Given any parameter space point in the mSUGRA model with typically too high a relic density, one can always *increase* m_ϕ beyond its mSUGRA value of m_0. A large value of $m_\phi > m_0$ implies via the RGEs and EWSB minimization conditions a smaller weak scale value of $|\mu|$, and thus the possibility of *mixed higgsino dark matter* with a WMAP-allowed relic density (as in the mSUGRA HB/FP region), even though m_0 is not large. Alternatively, if m_ϕ is negative, the value of $|\mu|$ increases, but m_A decreases: thus, by dialing m_ϕ to a sufficiently negative value, we can get *A-funnel annihilation, for any value of* $\tan\beta$.

In figure 6, we show curves which illustrate the value of δ_ϕ needed to move the mSUGRA relic density prediction into accord with (1.1), either by raising δ_ϕ or equivalently, m_ϕ, as in frame *a*), or by lowering δ_ϕ (and hence m_ϕ), to negative values as in frame *b*). We show curves versus m_0 for $m_{1/2} = 200$, 300 and 500 GeV, and for $A_0 = 0$, $\tan\beta = 10$ and 40 and $\mu > 0$. Curves terminate at both ends where we reach an end of the scanned m_0 space or hit a forbidden region. At the low m_0 end, no dialing of δ_ϕ is needed, since we are in the narrow stau co-annihilation region, or for $m_{1/2} = 200$ GeV, in
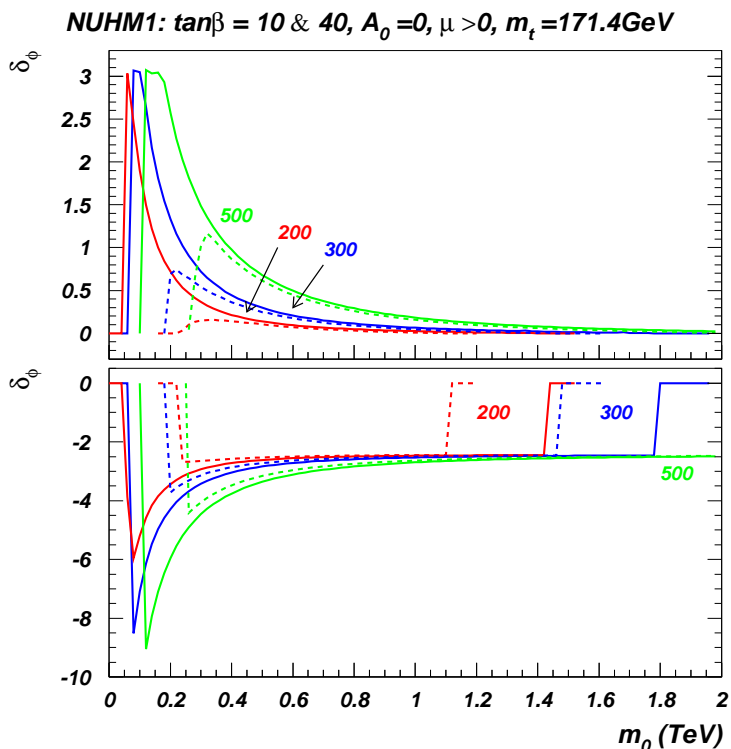
Figure 6: The values of δ_ϕ needed to bring various mSUGRA points into accord with the measured relic density versus m_0 for $A_0 = 0$ and $\tan\beta = 10$ (solid lines) and 40 (dashed lines) in the NUHM1 model. The curves correspond to $m_{1/2}$ values of 200, 300 and 500 GeV.

the bulk region. When we move to larger m_0, we eventually leave that region and large $|\delta_\phi|$ values become necessary to lower $|\mu|$ (or m_A). As we continue to increase m_0 in the upper frame, smaller values of δ_ϕ are necessary because of another assisting effect — the downward push of higgs mass-squared parameters from the top Yukawa coupling — is getting stronger. We smoothly reach the HB/FP region of mSUGRA where no dialing is required. The behaviour in the lower frame, where we adjust δ_ϕ so as to hit the Higgs-funnel region is qualitatively different at larger values of m_0: once we hit the HB/FP region, there is no need to have δ_ϕ different from zero. The jump in the curves reflects the rapidity with which this region is reached.

Implications for collider searches: in the case with $m_\phi > m_0$ where we have MHDM (even though m_0 can be much lower than its typical HB/FP value in mSUGRA), the low value of $|\mu|$ implies that *all* the charginos and neutralinos will be quite light. Thus, they are more likely to be seen either via direct -ino pair production at the LHC, or to be produced at large rates in gluino and squark cascade decays. In general, for small $|\mu|$, $\tilde{g}$ and $\tilde{q}$ cascade decay patterns become much more complex because many squark and gluino decay chains that are normally suppressed in the mSUGRA case become relevant. In addition, for small $|\mu|$, there is a smaller $\widetilde{Z}_2 - \widetilde{Z}_1$ mass gap, so $\widetilde{Z}_2$ 2-body "spoiler decays" $\widetilde{Z}_2 \to \widetilde{Z}_1 Z$ and $\widetilde{Z}_2 \to \widetilde{Z}_1 h$ are likely closed, and leptonic 3-body decays $\widetilde{Z}_2 \to \widetilde{Z}_1 \ell\bar{\ell}$ occur at observable

levels. The dilepton mass edge from these three-body decays frequently serves as the starting point for sparticle mass reconstruction in SUSY cascade decays at the LHC [32]. Since $|\mu|$ is small, it is also possible that $\widetilde{Z}_3$ also only decays via three-body channels. In this case, the dilepton mass distribution will contain three mass edges (though these may not all be observable), and its shape may provide further information about the nature of the neutralinos.

In the case where $m_\phi < 0$ so that $m_A \sim 2m_{\widetilde{Z}_1}$, A as well as the other heavier Higgs bosons H and $H^\pm$ are much lighter than expected in mSUGRA, even at low-to-moderate $\tan\beta$ values. In this case — for a fixed value of $\tan\beta$ — direct detection of the heavier Higgs states A, H and $H^\pm$ at the LHC is more likely than in mSUGRA, and further, these states may also be produced in the gluino and squark decay chains via the decays of secondary chargino and neutralinos [42].

Implications for DM searches: for the case of $m_\phi \gg m_0$ with small $|\mu|$ and MHDM, the enhanced higgsino component of the $\widetilde{Z}_1$ leads to *both* enhanced direct and indirect DM detection rates compared to mSUGRA. This case has excellent detection prospects in the next generation of detectors such as XENON-100, LUX or mini-CLEAN.

For the case where $m_\phi < 0$ with $m_A \sim 2m_{\widetilde{Z}_1}$, the $\widetilde{Z}_1$ remains nearly pure bino, so direct detection rates and indirect detection via neutralino annihilation to neutrinos in the solar core remain low, at values typical of mSUGRA models. However, indirect $\widetilde{Z}_1$ detection via halo annihilations to gamma rays or anti-matter are all enhanced relative to mSUGRA (but not always to observable levels), since the halo neutralinos can still annihilate through the s-channel pseudoscalar resonance [43].

2.2.3 Non-universal Higgs mass: two extra parameters case

Motivation: in susy GUT models based upon the gauge group SU(5), each of the MSSM Higgs superfields lives in *different* representations of the gauge group: $H_u \in \mathcal{H}_5$, while $H_d \in \mathcal{H}_{5^*}$. The two-extra-parameters NUHM model (NUHM2) [22] assumes independent Higgs field soft masses $m^2_{H_u}$ and $m^2_{H_d}$. The simplest assumption for the matter scalars is that they all acquire a common GUT scale mass m_0, although they also would exist in separate 5^* and 10 dimensional representations under SU(5).

Parameter space: one form of parameter space for the NUHM2 model is

$$m_0, \; m^2_{H_u}, \; m^2_{H_d}, \; m_{1/2}, \; A_0, \; \tan\beta, \; sign(\mu) \quad \text{(NUHM2}').\tag{2.3}$$

However, the EWSB minimization conditions allow the new GUT scale parameters $m^2_{H_u}$ and $m^2_{H_d}$ to be traded for the weak scale parameters $|\mu|$ and m_A which are frequently easier to work with for phenomenological analyses:

$$m_0, \; \mu, \; m_A, \; m_{1/2}, \; A_0, \; \tan\beta, \; sign(\mu) \quad \text{(NUHM2)}.\tag{2.4}$$

Both forms of parameter space are allowed in Isajet spectra and event generation. In addition, Blazek et al. [44] adopt a Higgs SSB parameterization wherein the Higgs soft
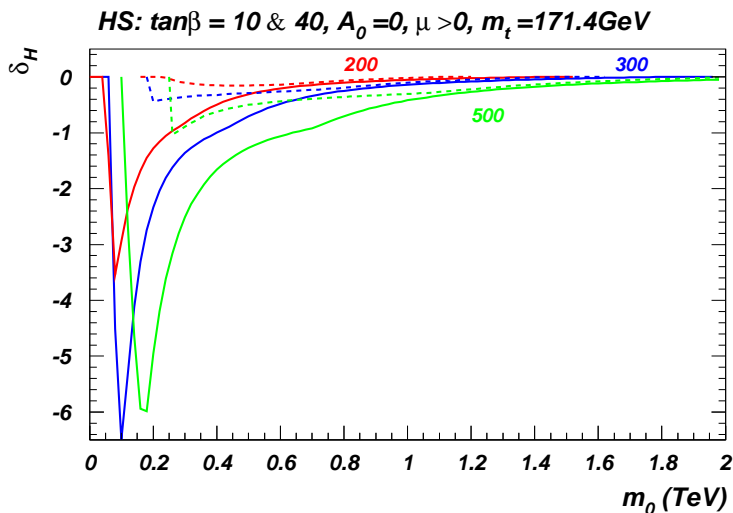
Figure 7: Values of δ_H needed to bring various mSUGRA points into accord with the measured relic density versus m_0 for $A_0 = 0$ and $\tan\beta = 10$ (solid lines) and 40 (dashed lines) in the NUHM2 HS scenario. The curves correspond to $m_{1/2}$ values of 200, 300 and 500 GeV.

masses are split evenly about a common mass which most generally is an independent parameter, m_{10}. Their parameterization is given by:

$$m_{H_{u,d}}^2 = m_{10}^2 \ (1 \mp \delta_H), \tag{2.5}$$

where δ_H is dimensionless and can take either positive or negative values. If we choose $m_{10} = m_0$, we obtain a one-parameter extension that we refer to as the Higgs-splitting (HS) model.

In figure 7, we illustrate the values of δ_H needed to move the mSUGRA relic density prediction into accord with (1.1) by lowering δ_H to negative values. This case gives rise to models with low μ *and* low m_A in the HS model. We show curves of $\delta_H < 0$ needed to pull the mSUGRA relic density into accord with eq. 1.1 versus m_0 for $m_{1/2} = 200$, 300 and 500 GeV, and for $\tan\beta = 10$ and 40, with $A_0 = 0$ and $\mu > 0$. Here the situation is similar to the NUHM1 case in that less dialing is required from larger m_0 due to the increasing top Yukawa coupling effect. As in the previous figure, less dialing is needed for the larger value of $\tan\beta$. We also mention that if instead δ_H is raised to large positive values (not shown in the figure), then instead one enters a WMAP-allowed region via $\tilde{\ell}_L/\tilde{\nu}$ or $\tilde{u}_R/\tilde{c}_R$ co-annihilation as discussed in ref. [22].

Implications for collider searches: in the NUHM2 model, since μ and m_A are free parameters, one is free to choose *both* μ and m_A to be small, so one can have MHDM and A-funnel annihilation contributions simultaneously. This type of model leads to the possibility of having light -inos *and* light A, H and $H^\pm$ at the same time. This would lead to a very complex and rich pattern of gluino and squark cascade decays at the LHC.

A new distinct possibility also arises in the NUHM2 model. In the MSSM scalar mass

RGEs (see e.g. Ch. 9 of ref. [2]), the right-hand-side includes a term

$$S = m_{H_u}^2 - m_{H_d}^2 + Tr\left[\mathbf{m}_Q^2 - \mathbf{m}_L^2 - 2\mathbf{m}_U^2 + \mathbf{m}_D^2 + \mathbf{m}_E^2\right]$$

which vanishes in the mSUGRA case, but is obviously non-zero if the Higgs soft masses are split. If the Higgs mass splitting is large, then the S-term helps push the m_L^2 and m_U^2 soft terms to small values, leading to cases with left-slepton neutralino co-annihilation, or to cases with very light $\tilde{u}_R$ and $\tilde{c}_R$ squark masses, with squark-neutralino co-annihilation acting to reduce the relic density. The presence of very light left-sleptons or light $\tilde{u}_R$, $\tilde{c}_R$ squarks, with other sfermions at the TeV scale, might be an indication of the HS scenario with large, positive $\delta_H > 0$. In this case, contrary to the prediction of many models, the lighter stau is dominantly $\tilde{\tau}_L$.

Implications for DM searches: for the NUHM2 model, all direct and indirect DM detection rates are strongly enhanced if μ is small, while only halo annihilation rates are enhanced if $2m_{\widetilde{Z}_1} \sim m_A$. If instead parameters are in the region where agreement with the observed relic density occurs because the left-type sleptons are relatively light, we do not expect increases in either direct or indirect detection rates. Finally, in the light $\tilde{u}_R$, $\tilde{c}_R$ region, rates for direct detection of DM, as well as for its indirect detection via observation of high energy $\tilde{\nu}_\mu$'s at IceCube will be enhanced since these depend mainly on neutralino-nucleon scattering via squark exchange, and $\tilde{u}_R$ squarks are light. Halo annihilation rates are also somewhat enhanced, since neutralinos can more easily annihilate into $u\bar{u}$ and $c\bar{c}$ pairs, giving rise to gamma ray and anti-matter signals [22].

2.3 Models with non-universal gaugino masses

Motivation: in mSUGRA, it is assumed that the gaugino mass parameters M_1, M_2 and M_3 unify to $m_{1/2}$ at $Q = M_{\rm GUT}$. This holds true in supergravity models if the gauge kinetic function $f_{AB} \sim \delta_{AB}f(h_M)$, where A, B are gauge indices, and $f(h_M)$ is an arbitrary function of hidden sector fields h_M, but common to all the gauge groups. More generally, the gauge kinetic function need only transform at the symmetric product of two adjoints. In this more general case, if the auxiliary field that breaks supersymmetry also breaks the grand unification gauge symmetry, GUT scale gaugino mass parameters need not unify [45]. Non-unified masses also occur in models of gaugino-mediated SUSY breaking [46] and in various string-motivated models [47]. In models with mixed moduli-anomaly mediated SUSY breaking (MMAMSB) [48], the gaugino masses are again split at $M_{\rm GUT}$, with the splitting proportional to the gauge group β-functions. Motivated by these considerations, in the phenomenological models that we consider below, we will allow independent gaugino mass parameters at $Q = M_{\rm GUT}$. To isolate the effect, we will assume that just one of these mass parameters deviates from it unified value, and tune it to reproduce the measured value of the DM relic density leaving the other two at $m_{1/2}$.

2.3.1 Mixed wino dark matter

Parameter space: in mSUGRA, at the GUT scale one assumes $M_1 = M_2 \equiv m_{1/2}$ which leads to $M_1 \sim \frac{M_2}{2}$ at the weak scale due to RG running. The $\widetilde{Z}_1$ is usually a nearly pure

bino state with too large a relic density. In anomaly-mediated SUSY breaking (AMSB) models [49], the $\widetilde{Z}_1$ is nearly pure wino-like, with too low a relic density. There exists, therefore, an intermediate situation with $M_1 \sim M_2$ at the weak scale which gives the observed relic density, so that the $\widetilde{Z}_1$ is *mixed wino dark matter* (MWDM) [23]. Starting from the mSUGRA model boundary conditions at $M_{\rm GUT}$, one can either increase M_1 so that $M_1 > M_2 = M_3 = m_{1/2}$:

$$m_0, \ M_1, \ m_{1/2}, \ A_0, \ \tan\beta, \ sign(\mu) \quad \text{(the MWDM1 case)} \tag{2.6}$$

or lower M_2 such that $M_2 < M_1 = M_3 = m_{1/2}$:

$$m_0, \ M_2, \ m_{1/2}, \ A_0, \ \tan\beta, \ sign(\mu) \quad \text{(the MWDM2 case)}. \tag{2.7}$$

In the MWDM1 case, since M_1, M_2 and μ will all be much closer together, the $\widetilde{Z}_1$ is actually a mixed bino-wino-higgsino state, while in MWDM2, since $M_1 \sim M_2 \ll \mu$, the $\widetilde{Z}_1$ is more a pure bino-wino mixed state.

In figure 8, we show curves which illustrate the GUT scale ratio of $r_1 = M_1/m_{1/2}$ needed to move the mSUGRA relic density prediction into accord with (1.1). We show curves versus m_0 for $m_{1/2} = 200$, 300 and 500 GeV, and for $\tan\beta = 10$ and 40. We take $A_0 = 0$ and $\mu > 0$. At the lowest m_0 values $r_1 = 1$ since we are in the stau co-annihilation (or for $m_{1/2} = 200$ GeV in the bulk) region. For m_0 values beyond this, we have to dial M_1 so as to obtain a mixed bino-wino-higgsino $\widetilde{Z}_1$ to be in concordance with the observed relic density measurement. For very large values of m_0 approaching the HB/FP region, the required value of r_1 once again begins to reduce as long as $m_{\widetilde{Z}_1} > M_W$ so that $\widetilde{Z}_1\widetilde{Z}_1 \to W^+W^-$ is accessible in the early universe . The up-turn in the $m_{1/2} = 200$ GeV curves at large values of m_0 occurs when this reaction becomes kinematically suppressed: in this case, a larger value of r_1 once again allows this reaction without which the relic density tends to be too large. However, for $m_{1/2} = 200$ GeV and $\tan\beta = 10$, and $m_0 \gtrsim 1.45$ TeV, we are deep enough into the HB/FP region so that even for mSUGRA the annihilation cross section via Z^* exchange is large enough to get agreement with (1.1) even with $m_{\widetilde{Z}_1} < M_W$.[4] In the case of the curves for $m_{1/2} = 300$ and 500 GeV, $m_{\widetilde{Z}_1}$ always remains above M_W so that the HB/FP region of mSUGRA is smoothly reached. The dashed curves exhibit analogous behaviour.

Implications for collider searches: in MWDM models with $M_1 \sim M_2$ such that the relic density constraint (1.1) is fulfilled, the mass gap $m_{\widetilde{Z}_2} - m_{\widetilde{Z}_1}$ generally tends to be $\sim 20-30$ GeV for MWDM2 models (larger for MWDM1, where the neutralino also has a higgsino component), somewhat smaller than the mass gap of ~ 50 GeV found in models with MHDM (such as the HB/FP region of mSUGRA). This means that at collider experiments, the same-flavor/opposite-sign isolated dilepton mass spectrum should have a single visible edge around 20-30 GeV arising from $\widetilde{Z}_2 \to \widetilde{Z}_1\ell\bar{\ell}$ decays. Moreover, the shape of the dilepton spectrum should correspond to one where the neutralino eigenvalues have the same sign. This should be distinct from MHDM models which tend to have the higher

---

[4]This portion of the curve is excluded by the LEP constraint on $m_{\widetilde{W}_1}$.

MWDM1: tanβ **= 10** & **40,** A_0 **=0,** μ **>0,** m_t **=171.4GeV**
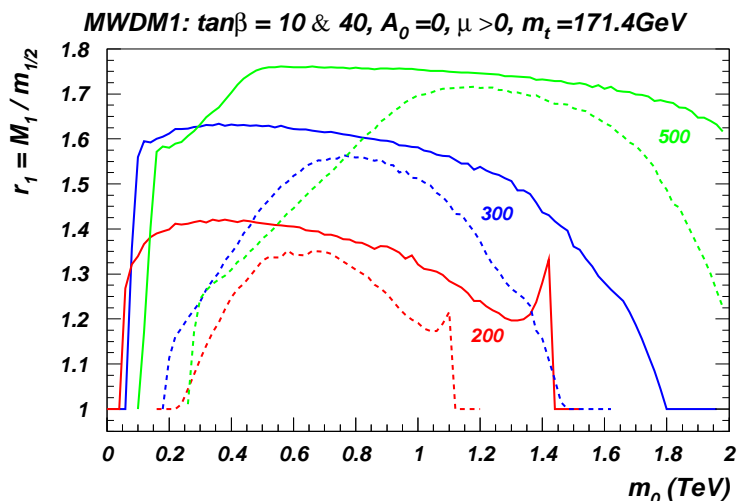
Figure 8: Values of $r_1 = M_1/m_{1/2}$ needed to bring various mSUGRA points into accord with the measured relic density versus m_0 for $A_0 = 0$ and $\tan\beta = 10$ (solid lines) and 40 (dashed lines) in the MWDM1 scenario. The curves correspond to $m_{1/2}$ values of 200, 300 and 500 GeV. For the 200 (300) GeV solid curves, the regions with $m_0 \gtrsim 1.4$ (1.94) TeV are excluded because the chargino is too light.

mass edge and possibly a shape corresponding to opposite signs of the neutralino mass eigenvalues [50]. Also since MHDM models have a small μ parameter, edges due to $\widetilde{Z}_3$ decay may also be visible. The small $\widetilde{Z}_2 - \widetilde{Z}_1$ mass gap suppresses 3-body decays of $\widetilde{Z}_2$ more than 2-body decays: then the branching fraction for the radiative decay $\widetilde{Z}_2 \to \widetilde{Z}_1\gamma$, which is normally very suppressed in mSUGRA, can reach the 10% level in the MWDM models [24, 51]. Finally, when M_1 is raised, it feeds into raising masses of especially right-type sleptons relative to their mSUGRA predictions. Likewise, when M_2 is reduced, left-squark and slepton masses get reduced relative to mSUGRA.

Implications for DM searches: in the MWDM1 scenario, the $\widetilde{Z}_1$ becomes a mixed bino-wino-higgsino state, and as a result all direct and indirect DM detection rates are boosted relative to mSUGRA — sometimes by an order of magnitude or more due to the enhanced higgsino component. In the MWDM2 scenario, where the $\widetilde{Z}_1$ develops a smaller higgsino component, direct detection and ν_μ indirect detection rates are only slightly enhanced, while indirect DM detection rates from halo annihilations can again be boosted by an order of magnitude or more, but not necessarily to observable levels.

2.3.2 Bino-wino co-annihilation (BWCA)

Parameter space: in the BWCA scenario [24], where $M_1 \sim -M_2$ at the weak scale, there is very little mixing between the bino and neutral wino states even when these are very close in mass. If $|M_1|$ is just slightly smaller than $|M_2|$, and $|\mu|$ is relatively large, the lightest neutralino remains bino-like, but because $m_{\widetilde{Z}_1} \simeq m_{\widetilde{Z}_2, \widetilde{W}_1}$, bino-wino co-annihilation processes in the early universe reduce the relic density to the observed level. In the BWCA case, the parameter space is the same as in the MWDM case, except that M_1 and M_2 are

now opposite in sign. As with the MWDM case, one can either raise $|M_1|$ by about a factor 2, or lower $|M_2|$ by about the same factor to attain $-M_1 \sim M_2$ at the weak scale.

In figure 9, we show curves which illustrate the GUT scale ratio $r_2 = M_2/m_{1/2}$ needed to move the mSUGRA relic density prediction into accord with (1.1). We show results versus m_0, for $m_{1/2} = 200$, 300 and 500 GeV, and for $\tan\beta = 10$ and 40. We take $A_0 = 0$ and $\mu > 0$ (upper frame) and $\mu < 0$, the sign favored by the E821 $(g-2)_\mu$ experiment (lower frame), at least for lower ranges of m_0 and $m_{1/2}$. That the ratio r_2 remains close to $-1/2$ in the upper frame, for all m_0 values in between the stau-coannihilation and the HB/FP regions, reflects the fact that the evolution of gaugino masses does not depend on sfermion masses at 1-loop. The solid lines for $\tan\beta = 10$ in the lower frame show very similar behaviour, except that μ is now negative. In contrast, there is a large flat region at low values of m_0 in the $\tan\beta = 40$ case shown by the dashed lines. We have traced this to the fact that the Higgs funnel region has already opened up even for $\tan\beta = 40$, and that the funnel region is contiguous to the stau co-annihilation (and for $m_{1/2} = 200$ GeV, also the bulk) region.

Implications for collider searches: in the BWCA scenario, the $\widetilde{Z}_2 - \widetilde{Z}_1$ mass gap becomes very small: of order 15-30 GeV typically. Thus, as in the MWDM case, one expects a $m(\ell\bar{\ell})$ mass edge to be visible owing to $\widetilde{Z}_2 \to \widetilde{Z}_1 \ell\bar{\ell}$ decay, since all $\widetilde{Z}_2$ two-body spoiler decay modes are kinematically closed. The mass gap should be much smaller than that typically expected from mSUGRA models. The $m(\ell^+\ell^-)$ distribution for opposite-sign/ same flavor dileptons should contain a single mass-edge, "one hump bump", unlike the case of MHDM, which favors a "two-hump-bump" since $\widetilde{Z}_3$ would be light as well.[5]

The small mass gap (required for effective co-annihilation) strongly favors two-body decays over three-body decays and results in large branching fraction for the radiative decay $\widetilde{Z}_2 \to \widetilde{Z}_1 \gamma$: reaching over 30% in the scans presented in ref. [24]. If $\widetilde{Z}_2$ were at rest, the γ from the radiative decay would be mono-energetic but rather soft. However, for fast moving $\widetilde{Z}_2$ secondaries from gluino and squark cascade decays, the photon energy gets boosted, and in the BWCA case there should be an observable signal also in the multi-jet plus isolated photon plus E_T^{miss} channel at the LHC: see figure 16 of ref. [24].

At e^+e^- colliders, the relative minus sign between M_1 and M_2 leads to enhanced production of $\widetilde{Z}_1 \widetilde{Z}_2$ pairs compared to mSUGRA predictions, and also the predictions in the MWDM case. This provides a way of distinguishing between the BWCA and MWDM frameworks which otherwise have a very similar mass spectrum. Moreover, operating just above $\widetilde{Z}_1 \widetilde{Z}_2$ threshold, one might make detailed studies of $\widetilde{Z}_2$ decay branching fractions, including the radiative mode $\widetilde{Z}_2 \to \widetilde{Z}_1 \gamma$, which will result in events with almost mono-energetic single photons recoiling against "nothing".

Implications for DM searches: in the BWCA case, since the $\widetilde{Z}_1$ remains purely bino-like, rates for indirect DM detection remain low, similar to results from the corresponding mSUGRA case in many instances. Rates for direct DM detection can be far below the sensitivity of any proposed detector if the sign of $M_1\mu$ is negative, i.e. for $\mu > 0$ in the

---

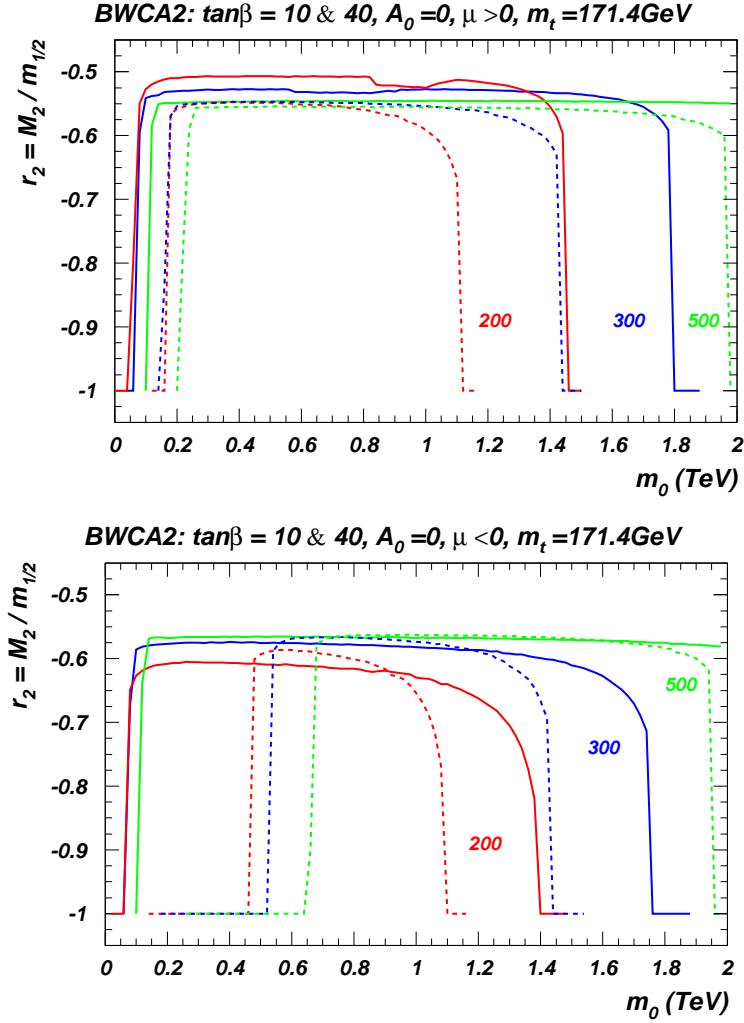[5]We thank Dr. Theodore Geisel for coining related expressions.

Figure 9: Values of $r_2 = M_2/m_{1/2}$ needed to bring various mSUGRA points into accord with the measured relic density versus m_0 for $A_0 = 0$ and $\tan\beta = 10$ (solid lines) and 40 (dashed lines) in the BWCA scenario. The upper frame is for $\mu > 0$ while in the lower frame we take $\mu < 0$. The curves correspond to $m_{1/2}$ values of 200, 300 and 500 GeV.

BWCA2 case, and for $\mu < 0$ in the BWCA1 case, because of cancellations in neutralino couplings that enter the direct DM detection rate calculations [24].

2.3.3 Low $|M_3|$ dark matter: compressed SUSY

Parameter space: the low $|M_3|$ dark matter (LM3DM) scenario arises by starting with mSUGRA parameter space, but (for $m_0 \lesssim 1 - 2\,\text{TeV}$) *lowering* the GUT scale value of $|M_3|$ relative to $M_1 = M_2 = m_{1/2}$ [52, 25]. Lowering $|M_3|$ results in smaller gluino and, via RGE effects, also squark masses. These effects feed into the MSSM RGEs and affect the running of $m_{H_u}^2$ – effectively diminishing the downward push from the top quark Yukawa coupling — resulting in lower $|\mu|$ values, and hence MHDM. The MHDM case can be easily compatible with the observed relic density constraint since there is enhanced neutralino

annihilation to WW, ZZ and Zh states in the early universe. Thus, the parameter space is given by

$$m_0, \ m_{1/2}, \ M_3, \ A_0, \ \tan\beta, \ sign(\mu) \quad \text{(the LM3DM case)}. \qquad (2.8)$$

Here, M_3 can be of either sign. Although the first and second generation sfermion masses are essentially unaffected by the sign flip, $m_{\tilde{t}_1}$, and through μ, also chargino and neutralino masses, do show clear dependence on the relative sign between M_3 and $M_{1,2}$.

In figure 10, we show the GUT scale ratio of $r_3 = M_3/m_{1/2}$ needed to move the mSUGRA relic density prediction into accord with (1.1) versus m_0. As always, we show results for $m_{1/2} = 200$, 300 and 500 GeV, and for $\tan\beta = 10$ and 40. We take $A_0 = 0$ and $\mu > 0$. For the solid curves, we see that once we are away from the stau co-annihilation (and for the $m_{1/2} = 200$ GeV case, also bulk) region, we need to reduce $|M_3(\mathrm{GUT})|$ to obtain the correct relic density. Since in this scenario we are lowering μ, the degree of dialing is generally smaller for larger m_0 due to increasing top Yukawa coupling effects, just as in the NUHM1 model with positive δ_ϕ. The situation is more complicated for the dashed curves where $\tan\beta = 40$. For $M_3 < 0$, the Higgs funnel already starts to appear for this relatively low value of $\tan\beta$. For the red and blue dashed curves corresponding to $m_{1/2} = 200$ and 300 GeV, respectively, this funnel region is contiguous with the bulk/stau co-annihilation region, so that r_3 remains at -1 for $m_0 \lesssim 600$ GeV. For yet larger values of m_0, $|r_3|$ needs to be dialed down though, because of the proximity of the Higgs funnel, by not quite as much as for the corresponding $\tan\beta = 10$ case, until the HB/FP region is reached. For the $m_{1/2} = 500$ GeV curve, the Higgs-funnel region occurs for 450 GeV $\lesssim m_0 \lesssim 800$ GeV, and is well separated from the stau co-annihilation region. Thus some tuning of r_3 (but again, not as much as in the $\tan\beta = 10$ case) is needed for m_0 values away from the very narrow stau co-annihilation region, and again for large m_0 values outside the Higgs-funnel region, until the HB/FP region is reached at $m_0 \sim 1.9$ TeV. For $M_3 > 0$, although the Higgs-funnel does not occur for $\tan\beta = 40$, s-channel A/H exchange does significantly enhance neutralino annihilation amplitudes for $m_0 \lesssim 2m_{1/2}$: as a result, the value of r_3 needed varies more slowly at the low m_0 end for the dashed curves than for the solid curves.

We should mention that a related scenario, dubbed "compressed SUSY", has been suggested by Martin [53]. In compressed SUSY, M_3 is lowered, but also by choosing large negative values of the A_0 parameter, a rather light $\tilde{t}_1$ state can be generated. Then if $m_{\widetilde{Z}_1} > m_t$, neutralino annihilation via $\widetilde{Z}_1\widetilde{Z}_1 \to t\bar{t}$, which does not suffer the usual P-wave suppression because of the large top quark mass, can dominate in the early universe, resulting in the observed relic density in a different way. The phenomenology of compressed SUSY models has been examined in ref. [54].

Implications for collider searches: since $m_{\tilde{g}}$ and $m_{\tilde{q}}$ are lowered relative to $m_{\widetilde{W}_1}$ values, the Tevatron and LHC reach is enhanced compared to corresponding mSUGRA predictions. In mSUGRA, the chargino mass limit $m_{\widetilde{W}_1} > 103.5$ GeV from LEP2 usually pre-empts the limit from direct gluino searches at the Tevatron because in models with gaugino mass unification, $m_{\tilde{g}} \sim 3.5 m_{\widetilde{W}_1}$, and thus $m_{\tilde{g}} \gtrsim 350$ GeV, which is not far from the reach of a 2 TeV $p\bar{p}$ collider. However, in LM3DM with non-unified gaugino masses,
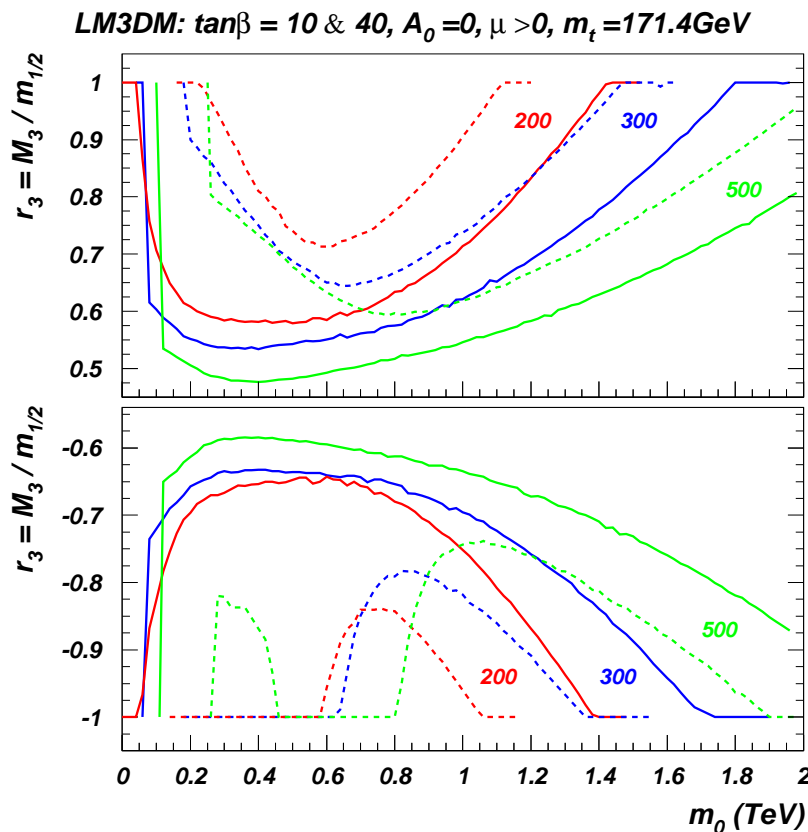
Figure 10: Values of the GUT scale ratio $r_3 = M_3/m_{1/2}$ needed to bring various mSUGRA points into accord with the measured relic density versus m_0 for $A_0 = 0$ and $\tan\beta = 10$ (solid lines) and 40 (dashed lines) in the LM3DM scenario. The curves correspond to $m_{1/2}$ values of 200, 300 and 500 GeV.

the gluino can have a mass as low as ~ 200 GeV, while the chargino remains in the LEP2 allowed region, $m_{\widetilde{W}_1} > 103.5$ GeV . Thus, a significant chunk of LM3DM parameter space is open to gluino pair and gluino-squark searches at the Tevatron [55]. Since the gluino mass is lowered with respect to $m_{\widetilde{Z}_1}$, the radiative gluino decay $\tilde{g} \to \widetilde{Z}_1 g$ may be the dominant decay mode of the $\tilde{g}$, with a branching fraction [56] as high as 85% in regions of parameter space where squarks are very heavy. In this case, the decay of a gluino leads to a single high p_T jet, and gluino pair production will look more like squark production.

Since the $\widetilde{Z}_1$ is MHDM in the LM3DM scenario, the $\widetilde{Z}_2 - \widetilde{Z}_1$ mass gap is again lowered compared to mSUGRA predictions, and the $\widetilde{Z}_2 \to \widetilde{Z}_1 \ell\bar{\ell}$ decay should be visible at LHC searches. In the LM3DM case, the mass gap is typically of order 30-80 GeV, and there should be $\widetilde{Z}_3$ contributions to the $m(\ell\bar{\ell})$ distribution as well, thus allowing the MHDM scenario to be distinguished from BWCA or MWDM. The large higgsino content of the neutralino $\widetilde{Z}_1$ will also tend to lead to a large branching ratio for gluino decays to third generation quarks so that the reach of the LHC will be enhanced by tagging b-jets [57].

For ILC searches, it is more likely that squark pair production (especially $\tilde{t}_1 \bar{\tilde{t}}_1$ production) will be accessible. In addition, since the $\widetilde{Z}_3$, $\widetilde{Z}_4$ and $\widetilde{W}_2$ states are lighter than the

corresponding mSUGRA parameter space points, it is more likely that various -ino pair production reactions would be accessible to ILC searches, allowing the reconstruction of chargino and neutralino mass matrices.

Implications for DM searches: in the LM3DM scenario, since we expect *both* light squarks and low μ (leading to MHDM), direct DM search rates are enhanced relative to mSUGRA by up to *two orders of magnitude*! Rates for ν_μ events at IceCube are enhanced by up to three orders of magnitude! Similar enhancements are seen in gamma ray and anti-matter search predictions arising from neutralino annihilation in the galactic halo. Thus, the LM3DM scenario seems a boon for direct and indirect DM searches.

2.3.4 High $|M_2|$ dark matter: left-right split SUSY

Parameter space: in the high $|M_2|$ dark matter scenario (HM2DM), the parameter set is the same as in the MWDM2 scenario, except that now the SU(2) gaugino mass parameter M_2 is dialed *up* in magnitude [26]. This increased value of $|M_2|$ feeds into the MSSM RGEs by first pushing $m_{H_u}^2$ to higher values (than in the universal gaugino mass case) during its evolution from $Q = M_{\mathrm{GUT}}$. Then as RG running continues, the top Yukawa coupling terms take over, and $m_{H_u}^2(Q)$ begins to be reduced. Since its positive peak-value was higher than in the canonical case with universal gaugino masses, $m_{H_u}^2$ attains a relatively small negative value when the evolution is stopped at the weak scale. Finally, since $\mu^2 \sim -m_{H_u}^2(\mathrm{weak})$, we end up with a small weak scale $|\mu|$ parameter, and MHDM.

In the HM2DM scenario, the large value of $|M_2(M_{\mathrm{GUT}})|$, via RG evolution, lifts the SSB masses of SU(2) doublet matter scalars to large values, so that left-sleptons, and to a smaller extent also left-squarks, are much heavier than right- ones. Thus, the HM2DM model can be regarded as left-right split SUSY. In this model, all light third generation matter sfermions $(m_{\tilde{f}_1})$ then tend to be predominantly right- states, whereas in most models, the $\tilde{b}_1$ tends to be mainly $\tilde{b}_L$, and $\tilde{t}_1$ tends to be a mixed left-right squark state. Further, since $|\mu|$ is small, the HM2DM model leads to a spectrum with light $\widetilde{Z}_1$, $\widetilde{Z}_2$, $\widetilde{Z}_3$ and $\widetilde{W}_1$ states, which tend to be higgsino-like or mixed bino-higgsino. The $\widetilde{W}_2$ and $\widetilde{Z}_4$ are nearly pure winos, and also very heavy.

In figure 11, we show values of the GUT scale ratio of $r_2 = M_2/m_{1/2}$ needed to bring the neutralino relic density prediction into accord with (1.1). We show curves versus m_0 for $m_{1/2} = 200$, 300 and 500 GeV, for $\tan\beta = 10$ and 40, with $A_0 = 0$. Since $\Delta a_\mu^{\mathrm{SUSY}} \propto \mu M_2$ we take $sign(\mu) = sign(M_2)$ so their product is positive in accordance with the measured value of $(g-2)_\mu$ [37]. As in the LM3DM model, flipping the sign of M_2 (without changing its magnitude) causes the A-funnel to open up for $\tan\beta = 40$. But now the funnel region remains merged with the stau-coannihilation region even for $m_{1/2} = 500$ GeV, so that for the lower range of m_0 no additional dialing is necessary and r_2 remains at -1.

Implications for collider searches: in the HM2DM scenario, since we again have MHDM, the $\widetilde{Z}_2 - \widetilde{Z}_1$ mass gap tends to be in the range 30-80 GeV, so that the mass edge from $\widetilde{Z}_2 \to \widetilde{Z}_1 \ell\bar{\ell}$ decays, and possibly also from $\widetilde{Z}_3$ decays, should be seen in gluino and squark cascade decay events at the LHC. The shape of the distributions may also make it
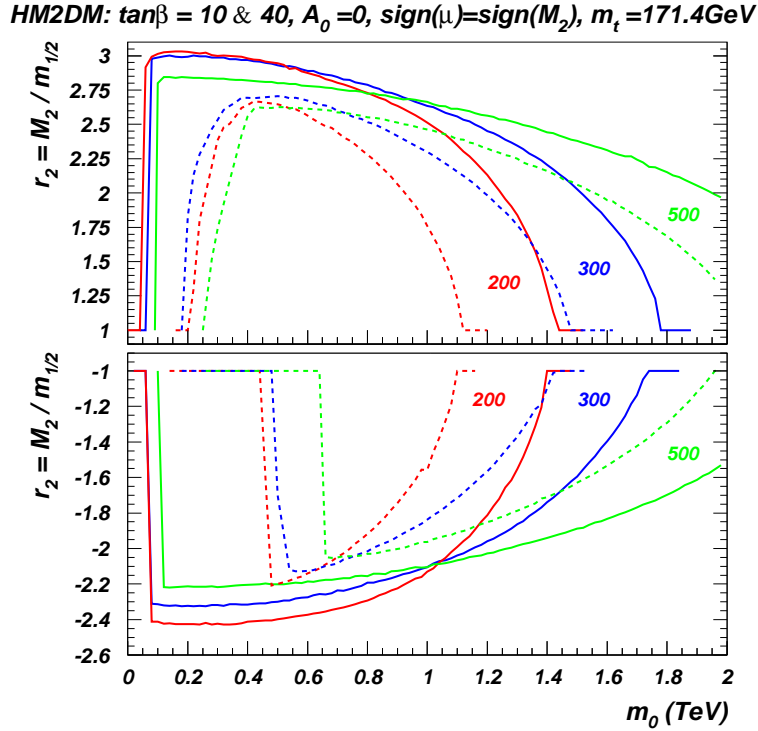
Figure 11: Values of the GUT scale ratio $r_2 = M_2/m_{1/2}$ needed to bring various mSUGRA points into accord with the measured relic density versus m_0 for $A_0 = 0$ and $\tan\beta = 10$ (solid lines) and 40 (dashed lines) in the HM2DM scenario. The curves correspond to $m_{1/2}$ values of 200, 300 and 500 GeV.

possible to glean information about the relative signs of the neutralino mass eigenvalues. Also, the increased higgsino content of the lighter states should again lead to increased b-jet multiplicity in SUSY events at the LHC.

At the ILC, the production of chargino and neutralino pairs would vary in a contrasting way compared to mSUGRA because the low lying gaugino states would be essentially devoid of wino components. If third generation squarks and sleptons are accessible to ILC searches, then a variation in beam polarization would reveal all these states to be predominantly right-type states, and their pair production cross sections would decrease with increasingly left-polarized beams.

Implications for DM searches: since in the HM2DM scenario, the $\widetilde{Z}_1$ is a mixed bino-higgsino state, its signal for spin-independent direct detection should be observable at the next generation of detectors (super-CDMS or 100 kg noble liquid detectors) over much of the parameter space. The ν_μ signal at IceCube or Antares would also be boosted by up to two orders of magnitude compared to mSUGRA and may be observable over a substantial portion of parameter space. Rates for detection of gamma rays and anti-matter from neutralino halo annihilation are also boosted relative to mSUGRA by 1-2 orders of magnitude.

3. Illustrative benchmark cases

In this section, we list some benchmark cases of models with universality and non-universality. We start with the mSUGRA model, and adopt a point in parameter space with

$$m_0, \ m_{1/2}, \ A_0, \ \tan\beta, \ sign(\mu) = 300 \text{ GeV}, \ 300 \text{ GeV}, \ 0, \ 10, \ +1$$

with $m_t = 171.4 \text{ GeV}$. This point is listed in column 2 of table 1. We see that we get $\Omega_{\widetilde{Z}_1} h^2 = 1.1$ for this point which is conclusively in conflict with (1.1), and so excluded assuming standard Big Bang cosmology and thermal relic neutralinos. For every other model in table 1, we relax the universality assumption and allow one additional parameter that we tune to bring the model into the DM-allowed range with $\Omega_{\widetilde{Z}_1} h^2 \sim 0.1$. The point here is to be able to compare and contrast the spectra along with other features of each of these DM-allowed models with the corresponding spectrum of the mSUGRA model, and with one another. We also list at the bottom the Isatools output of $\Omega_{\widetilde{Z}_1} h^2$, $BF(b \to s\gamma)$, the SUSY contribution to the muon anomalous magnetic moment $\Delta a_\mu^{\text{SUSY}}$, the spin-independent cross section for the elastic neutralino-proton scattering $\sigma_{\text{SI}}(\widetilde{Z}_1 p)$, and the Higgsino content of the neutralino $R_{\tilde{H}} = \sqrt{v_1^{(1)2} + v_2^{(1)2}}$ in the notation of ref. [2]. We use ISAJET 7.76 to generate this table.

In the first non-universal case, the NMH model, we see that the first/second generation SSB parameter $m_0(1,2) = 54 \text{ GeV}$ in order to obtain the observed relic density. Then, the $\tilde{e}_R$ and $\tilde{e}_L$ states (and also the $\tilde{\mu}_R$ and $\tilde{\mu}_L$ states) have much reduced masses than the corresponding mSUGRA case, while $m_{\tilde{\tau}_{1,2}}$, and also gluino, chargino and neutralino masses are essentially unchanged from their mSUGRA values. The low value of $m_{\tilde{e}_R} = 128.9 \text{ GeV}$ and 10.5 GeV mass gap between $\tilde{e}_R/\mu_R$ and $\widetilde{Z}_1$ ensure a high rate for neutralino annihilation and co-annihilation in the early universe. In addition, while $BF(b \to s\gamma)$ remains near the measured and SM value because third generation squarks and charged Higgs bosons are heavy, the value of $\Delta a_\mu^{\text{SUSY}}$ is enhanced, thus reconciling these two possibly disparate measurements.

The second non-universal case, labelled NUHM1$_\mu$, comes from the NUHM1 model where m_ϕ is dialed up to 549 GeV so that μ becomes small and we have mixed higgsino DM, even though m_0 is far smaller than in the mSUGRA HB/FP region. In this case, $m_{\widetilde{W}_1}$ has been reduced so much that the point is actually LEP2 excluded. Note that $R_{\tilde{H}}$ has risen to 0.84, signaling a higgsino-like $\widetilde{Z}_1$. The branching ratio for the decay $b \to s\gamma$ is slightly reduced. The salient feature is the direct detection cross section, which is now in the range of well-tempered neutralino models [28, 30] with MHDM, is 37 times higher than the corresponding mSUGRA value, and very close to the current 90% CL limit from Xenon-10 search [58].

The third non-universal case, labelled NUHM1$_A$, dials m_ϕ to -728 GeV, which raises μ to large values but lowers m_A to be just above $2m_{\widetilde{Z}_1}$ so that A-funnel annihilation reduces the relic abundance, even though $\tan\beta$ is not large. In this case, sfermions and lighter -inos have essentially the same masses as in mSUGRA, but now we have relatively light Higgs

boson states A, H and $H^{\pm}$ accessible to LHC searches. Also, $BF(b \to s\gamma)$ is somewhat enhanced due to the light $H^{\pm}$ entering the $tH^{\pm}$ loop contribution to this decay.

The fourth non-universal case is the HS model and has the two Higgs soft masses split about the common value m_0, and has both MHDM and some A-funnel annihilation, with a light spectrum of Higgs bosons, as well as charginos and neutralinos. All the Higgs bosons and all the charginos and neutralinos should be accessible at an electron-positron collider operating at a center of mass energy just above $500\,$GeV. The higgsino component of the $\widetilde{Z}_1$, which is larger than in mSUGRA, leads to considerable enhancement of the direct detection cross section.

In table 2, we continue this comparison with the same mSUGRA point in table 1, but this time for models with non-universal gaugino mass parameters. We show the results for this mSUGRA point once again for the convenience of the reader. In column 3, we consider the MWDM1 model where we raise the GUT scale value of M_1 to $490\,$GeV, resulting in a $\widetilde{Z}_1$ state that is a mixed bino-wino-higgsino state. The heightened wino and higgsino components of $\widetilde{Z}_1$ allow for enhanced $\widetilde{Z}_1\widetilde{Z}_1 \to W^+W^-$ in the early universe, thus putting the model into accord with the measured DM abundance. The model has direct detection rates enhanced by a factor ~ 7 over mSUGRA, to the 10^{-8} pb range. Except for $\widetilde{Z}_1$ which now has a mass of $195\,$GeV compared to $119\,$GeV in mSUGRA, the sparticle spectra are almost the same in the two cases. The heavier $\widetilde{Z}_1$ state implies that the $\widetilde{Z}_2 - \widetilde{Z}_1$ mass gap is about $29\,$GeV compared to $\sim 100\,$GeV in mSUGRA, and that its higgsino-content is somewhat larger than in mSUGRA.

In the next column we consider a BWCA scenario where we dial $M_1(M_{\rm GUT})$ to $-480\,$GeV to obtain the observed relic density. Again, we see that except for $m_{\widetilde{Z}_1}$ which moves to $202\,$GeV, sparticle and Higgs boson masses as well as the higgsino content of the $\widetilde{Z}_1$ are essentially the same as for the corresponding mSUGRA model. The $\widetilde{W}_1 - \widetilde{Z}_1$ mass gap is now just $18\,$GeV, so bino-wino co-annihilation acts to reduce the relic density, even though the $\widetilde{Z}_1$ remains in a nearly pure bino-like state. The small $\widetilde{Z}_2 - \widetilde{Z}_1$ mass gap compared to the value of $m_{\widetilde{g}}$, which might be deduced at LHC, would signal a model with non-universal gaugino masses. Notice that for reasons detailed in ref. [30], the $\widetilde{Z}_1$ direct detection cross section is far lower than any proposed detector can probe.

In column 5, we attain the observed relic density by dialing $M_3(M_{\rm GUT})$ from $300\,$GeV to $160\,$GeV to obtain a viable LM3DM model. We see that we now have a much lighter spectrum of sparticles than in mSUGRA, not only squarks and gluinos, but also charginos and neutralinos (but not sleptons). In this case, we would expect huge sparticle production cross sections at LHC and complicated cascade decay chains. Since the reduction of M_3 hardly affects slepton masses, sleptons are not much lighter than squarks even though the sfermion mass scale is just 300-400 GeV. The $\widetilde{Z}_1$ has a significant higgsino content leading to MHDM with a $\widetilde{Z}_2 - \widetilde{Z}_1$ mass gap of $58\,$GeV, while the $\widetilde{Z}_3 - \widetilde{Z}_1$ mass gap is only slightly below M_Z, so 3-body $\widetilde{Z}_3$ decays will also occur, though the dilepton mass will be peaked close to M_Z. The large higgsino content also results in a correspondingly enhanced $\widetilde{Z}_1$ direct detection cross section — 7×10^{-8} pb — close to the 90% CL limit from Xenon-10 DM searches. We also see that the relatively light top squarks and charginos significantly reduce $BF(b \to s\gamma)$.

Model	mSUGRA	NMH	NUHM1$_\mu$	NUHM1$_A$	HS
parameter	—	$m_0(1,2)$	m_ϕ	m_ϕ	δ_H
special value	—	54	549	-728	-1.36
μ	385.1	386.5	105.8	748.5	269.3
$m_{\tilde{g}}$	729.7	722.1	731.4	733.4	728.9
$m_{\tilde{u}_L}$	720.8	658.4	724.3	720.5	720.1
$m_{\tilde{t}_1}$	523.4	526.5	484.1	624.5	505.8
$m_{\tilde{b}_1}$	656.8	659.8	642.2	689.5	645.4
$m_{\tilde{e}_L}$	364.5	216.2	364.8	365.8	373.4
$m_{\tilde{e}_R}$	322.3	128.9	322.5	321.9	301.8
$m_{\tilde{\tau}_1}$	317.1	317.6	317.8	316.4	299.3
$m_{\widetilde{W}_2}$	411.7	412.7	264.7	754.8	321.1
$m_{\widetilde{W}_1}$	220.7	219.5	91.1	234.9	196.6
$m_{\widetilde{Z}_4}$	412.5	413.5	268.1	754.6	322.9
$m_{\widetilde{Z}_3}$	391.3	392.7	137.3	747.1	277.1
$m_{\widetilde{Z}_2}$	220.6	219.4	117.4	234.5	198.1
$m_{\widetilde{Z}_1}$	119.2	118.4	69.0	121.5	115.4
m_A	520.3	521.9	584.5	268.5	279.0
m_{H^+}	529.8	531.4	593.8	281.6	292.0
m_h	110.1	110.1	109.8	110.5	109.8
$\Omega_{\widetilde{Z}_1} h^2$	1.1	0.10	0.11	0.11	0.10
$BF(b \to s\gamma) \times 10^4$	3.0	3.1	2.5	4.3	3.4
$\Delta a_\mu \times 10^{10}$	12.1	27.2	17.9	9.3	13.7
$\sigma_{\text{SI}}(\widetilde{Z}_1 p) \times 10^9$ (pb)	2.1	2.1	78	1.2	27
$R_{\tilde{H}}$	0.15	0.14	0.84	0.06	0.26

Table 1: A comparison of the characteristics of mSUGRA with corresponding characteristics in models with scalar mass non-universality that lead to the observed relic abundance of DM. Input parameters and resultant sparticle masses in GeV units, together with the predicted neutralino relic density, $BF(b \to s\gamma)$ and Δa_μ, the SUSY contribution to the anomalous magnetic moment of the muon, the direct detection cross section for the $\widetilde{Z}_1$, and finally, the higgsino content of the $\widetilde{Z}_1$. In each case, we fix $m_0 = m_{1/2} = 300$ GeV, $A_0 = 0$, $\tan\beta = 10$ and $m_t = 171.4$ GeV, and for each non-universal model tune the parameter in the first row to its special value shown in row 2 to reproduce the observed relic abundance.

Finally, in the last column in table 2, we show results for the HM2DM model where we get agreement with (1.1) by raising $M_2(M_{\text{GUT}})$ to 900 GeV. We see that this gives a very low value of μ so that the $\widetilde{Z}_1$ becomes MHDM with $R_{\tilde{H}} = 0.67$. We see that the left-type squarks and especially the left-type sleptons are now much heavier than in mSUGRA, while $\tilde{q}_R$ and $\tilde{\ell}_R$ are hardly affected, leading to the left-right split spectrum referred to earlier. The lighter chargino, and the three lightest neutralinos are all lighter than in mSUGRA, while $\widetilde{Z}_4$ is very heavy. The $\widetilde{Z}_2 - \widetilde{Z}_1$ mass gap is ~ 47 GeV, while the $\widetilde{Z}_3 - \widetilde{Z}_1$ mass gap is just 64 GeV. The branching ratio for $b \to s\gamma$ is reduced from its mSUGRA value

Model	mSUGRA	MWDM	BWCA	LM3DM	HM2DM
parameter	—	$M_1(M_{\rm GUT})$	$M_1(M_{\rm GUT})$	$M_3(M_{\rm GUT})$	$M_2(M_{\rm GUT})$
special value	—	490	-480	160	900
μ	385.1	385.9	376.6	185.3	134.8
$m_{\tilde{g}}$	729.7	729.9	731.7	420.2	736.4
$m_{\tilde{u}_L}$	720.8	721.2	722.0	496.9	901.8
$m_{\tilde{u}_R}$	702.7	708.9	709.9	467.0	696.3
$m_{\tilde{t}_1}$	523.4	526.5	536.3	312.2	394.3
$m_{\tilde{b}_1}$	656.8	656.0	658.9	443.2	686.4
$m_{\tilde{e}_L}$	364.5	371.5	371.4	366.1	669.3
$m_{\tilde{e}_R}$	322.3	353.3	352.2	322.6	321.3
$m_{\widetilde{W}_2}$	411.7	412.4	404.5	282.9	719.7
$m_{\widetilde{W}_1}$	220.7	220.8	220.0	152.5	136.5
$m_{\widetilde{Z}_4}$	412.5	414.5	403.3	285.2	723.1
$m_{\widetilde{Z}_3}$	391.3	391.9	385.8	194.4	160.2
$m_{\widetilde{Z}_2}$	220.6	223.2	219.2	163.6	142.3
$m_{\widetilde{Z}_1}$	119.2	194.6	201.7	105.5	94.8
m_A	520.3	525.9	518.6	398.3	670.7
m_{H^+}	529.8	535.3	528.1	408.7	679.8
m_h	110.1	110.2	109.8	106.0	111.9
$\Omega_{\widetilde{Z}_1}h^2$	1.1	0.10	0.10	0.10	0.10
$BF(b \to s\gamma) \times 10^4$	3.0	3.0	3.1	2.0	2.3
$\Delta a_\mu \times 10^{10}$	12.1	11.8	10.1	16.4	3.1
$\sigma_{\rm SI}(\widetilde{Z}_1 p) \times 10^9$ (pb)	2.1	15	0.031	72	34
$R_{\tilde{H}}$	0.15	0.25	0.16	0.50	0.67

Table 2: A comparison of the characteristics of mSUGRA with corresponding characteristics in models with gaugino mass non-universality that lead to the observed relic abundance of DM. Input parameters and resultant sparticle masses in GeV units, together with the predicted neutralino relic density, $BF(b \to s\gamma)$ and Δa_μ, the SUSY contribution to the anomalous magnetic moment of the muon, the direct detection cross section for the $\widetilde{Z}_1$, and finally, the higgsino content of the $\widetilde{Z}_1$. In each case, we fix $m_0 = m_{1/2} = 300\,{\rm GeV}$, $A_0 = 0$, $\tan\beta = 10$ and $m_t = 171.4\,{\rm GeV}$, and for each non-universal model tune the parameter in the first row to its special value shown in row 2 to reproduce the observed relic abundance.

because $\tilde{t}_1$ and the higgsino-like chargino are relatively light, while the DM direct detection cross-section is large, as is typical of models with MHDM.

4. General characteristics of relic-density-consistent models

In this section, we abstract general features of the various models that we have introduced earlier by performing scans over model parameters, where we keep only parameter points which lead to a relic density $\Omega_{\widetilde{Z}_1}h^2 \sim 0.11$. We also reject models with $m_{\widetilde{W}_1} < 103.5\,{\rm GeV}$ from LEP2 searches. In the case of the mSUGRA model, we scan parameters over the

range: $m_0 : 0 - 5\,\text{TeV}$, $m_{1/2} : 0 - 2\,\text{TeV}$, $A_0 = 0$, $\tan\beta = 10, 30, 45, 50, 52, 55$ and both signs of μ. Thus, our scans will include the stau co-annihilation region, the HB/FP region at large m_0 and the A-funnel at large $\tan\beta$. For models with non-universality, in order to have manageable parameter space scans, we restrict ourselves to a scan over mSUGRA parameters $m_0 : 0 - 2\,\text{TeV}$, $m_{1/2} : 0 - 1.5\,\text{TeV}$, $A_0 = 0$, $\tan\beta = 10$ and $\mu > 0$ (except for the HM2DM and BWCA2 models with negative M_2 where we take $\mu < 0$ since this is somewhat favored by the measurement of $(g - 2)_\mu$). For models with non-universality, for every set of mSUGRA parameters in our scan, we adjust the special additional parameter listed in the first rows of tables 1 and 2 to bring the neutralino relic density $\Omega_{\widetilde{Z}_1} h^2$ into accord with (1.1). Our upper limit on $m_{1/2}$ is chosen somewhat arbitrarily to avoid too much fine-tuning. We allow much larger values of m_0 just in the mSUGRA region, since in this case it has been argued that fine-tuning in the HB/FP region is not very large [11]. We limit ourselves to lower values of $m_0 < 2\,\text{TeV}$ in the models with non-universality since MHDM characteristic of the low $|\mu|$ values in the HB/FP region can be attained for all values of m_0.

4.1 Implications for collider searches

In figure 12 we show the value of $m_{\tilde{g}}$ vs. $m_{\tilde{u}_R}$ (as a representative value of the approximately degenerate squark mass) for both signs of mSUGRA, as well as for eight other models with non-universal SSB terms indicated in the legend on the figure. Each dot shows the gluino and up-squark mass for a model, with parameters chosen so that the neutralino relic density saturates (1.1). Notice that in this figure, as in several subsequent ones, not all the colors are visible since some model points are overwritten by other model points. The diagonal dashed line for $m_{\tilde{u}_R} = m_{\tilde{g}}$ shows that when we require that the observed relic density be obtained, with the exception of the two branches in the HB/FP region of mSUGRA where m_0 (and hence the squark mass) is very large, all models yield $m_{\tilde{g}} \sim m_{\tilde{q}}$. The two dotted lines denote the approximate reach of the CERN LHC with $100\,\text{fb}^{-1}$ of integrated luminosity if $m_{\tilde{g}} \simeq m_{\tilde{q}}$, as adapted from ref. [59]. Most of the models scanned lie within reach of the CERN LHC, which is partly an artifact from the upper limit we take on $m_{1/2}$ in our parameter space scans. For the two branches in the HB/FP region of mSUGRA shown by the red and blue dots at large m_0 in the figure, experiments at the LHC will be sensitive to models where $m_{\tilde{g}} \lesssim 1.8\,\text{TeV}$.

In figure 13, we show these DM-allowed models in the $m_{\tilde{t}_1}$ vs. m_h plane. Here, we note a clear trend in all models: heavier $\tilde{t}_1$ squarks are correlated with larger values of m_h, largely because top-Yukawa radiative corrections to m_h increase with the stop mass. For many models with $m_A \gg M_Z$, then $h \simeq H_{\text{SM}}$ so that the LEP2 lower bound of 114.1 GeV would be applicable. We have not required this bound in our analysis for reasons discussed earlier, and also to be able to show the trend of m_h with other observables. The lightest value of $m_{\tilde{t}_1}$ occurs in the LM3DM model, which allows $m_{\tilde{t}_1}$ as low as $\sim 200\,\text{GeV}$, although even lighter values of $m_{\tilde{t}_1}$ (readily accessible even at the Tevatron [60]) would be allowed if we also admitted variation of A_0.

In figure 14, we show the lighter chargino mass $m_{\widetilde{W}_1}$ vs. $m_{\widetilde{Z}_2} - m_{\widetilde{Z}_1}$. We denote by the dashed line the region where $m_{\widetilde{Z}_2} - m_{\widetilde{Z}_1} < M_Z$. Below this line, the spoiler decay

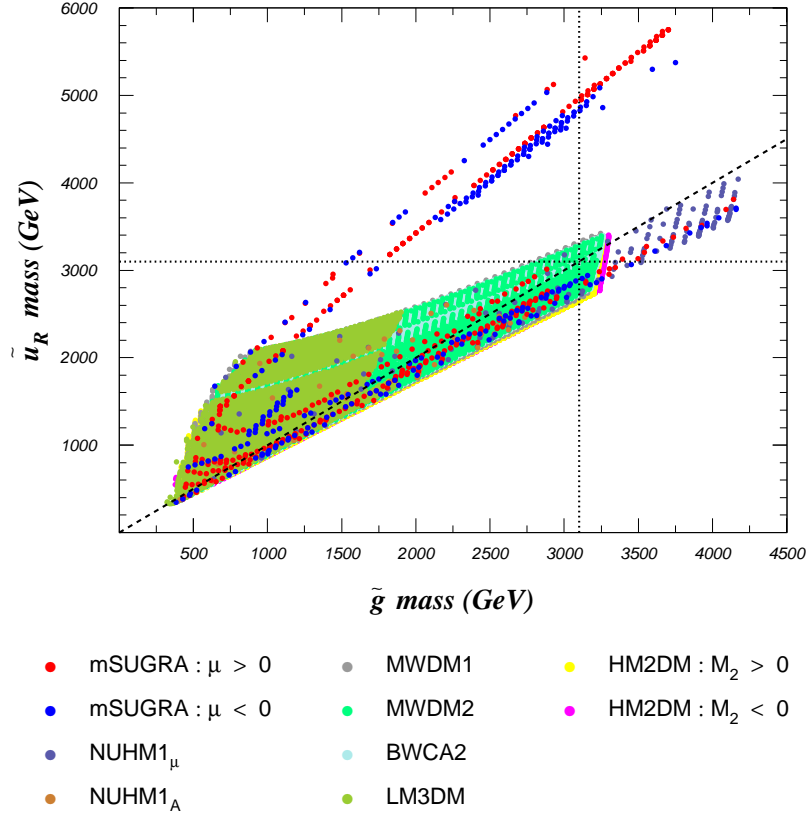**Figure 12:** Predictions for $m_{\tilde{g}}$ *vs.* $m_{\tilde{u}_R}$ from various models with $A_0 = 0$, $m_t = 171.4\,\mathrm{GeV}$ and $\mu > 0$ (except in the cases with the blue dots for the mSUGRA model, light blue dots for the BWCA2 model and magenta dots for the HM2DM model with $M_2 < 0$ for which we have $\mu < 0$), but where the special parameter in the various non-universal mass models has been dialed to yield $\Omega_{\widetilde{Z}_1} h^2 \simeq 0.11$. We fix $\tan\beta = 10$ except for the mSUGRA model where we allow $\tan\beta = 10$, 30, 45, 50, 52 and 55. The approximate $100\,\mathrm{fb}^{-1}$ reach of CERN LHC is denoted by the dotted lines, while a dashed line denotes where $m_{\tilde{u}_R} = m_{\tilde{g}}$. Here, and in subsequent figures, dots for some of the models are covered up by other dots, and so are not visible.

modes $\widetilde{Z}_2 \to \widetilde{Z}_1 Z$ or $\widetilde{Z}_1 h$ are kinematically closed, so that $\widetilde{Z}_2$ must decay via 3-body modes like $\widetilde{Z}_2 \to \widetilde{Z}_1 \ell\bar{\ell}$. The mass edge in the invariant dilepton mass distribution from this decay [32], which can serve as the starting point for sparticle mass reconstruction at the LHC as discussed earlier, will be visible as long as its branching fraction is not strongly suppressed [31]. From the figure, we see that *most* of the models that give rise to the correct relic density also predict that the spoiler modes are closed so that the $m(\ell\bar{\ell})$ mass edge will likely be visible! Exceptions arise from the stau-co-annihilation and A-funnel regions of mSUGRA, or at vestiges of other models which already had the correct relic
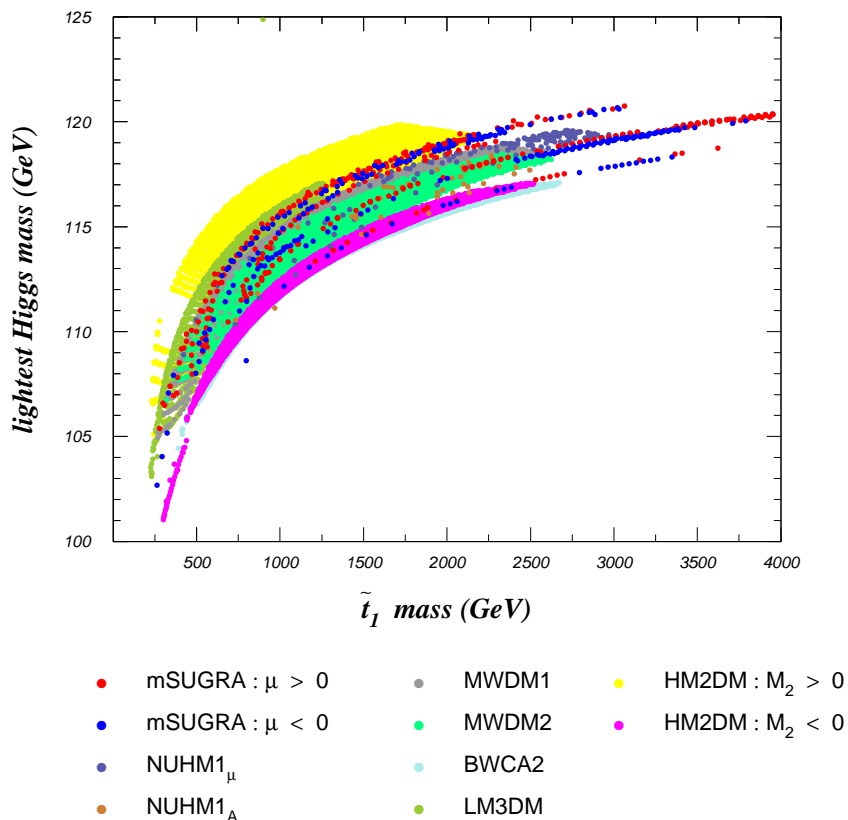
Figure 13: Predictions for m_h $vs.$ $m_{\tilde{t}_1}$ from various models with $A_0 = 0$, $m_t = 171.4\,\mathrm{GeV}$ and the sign of μ as in figure 12, but where the special parameter of non-universal mass models has been dialed to yield $\Omega_{\widetilde{Z}_1} h^2 \simeq 0.11$. We fix $\tan\beta = 10$ except for the mSUGRA model where we allow $\tan\beta = 10, 30, 45, 50, 52$ and 55.

density (because the mSUGRA parameters were in the stau co-annihilation region) so that no special non-universality parameters needed to be adjusted to get the correct relic density (e.g. the gray points from the MWDM1 model). Notice also that there are models where the mass gap is very small. Even for these models it is likely that the $\widetilde{Z}_2$ will be sufficiently boosted in its production via decays of much heavier squarks/gluinos so that the daughter leptons have large enough transverse momenta so as to be detectable.

In figure 15, we show predictions for $m_{\widetilde{W}_1}$ and $m_{\tilde{\tau}_1}$ for WMAP-allowed models. The approximate reach of the ILC500 ($\sqrt{s} = 500\,\mathrm{GeV}$) and ILC1000 (with $\sqrt{s} = 1000\,\mathrm{GeV}$) are shown by the dashed and dotted lines , respectively, which delineate the kinematic limit for $\widetilde{W}_1^+ \widetilde{W}_1^-$ or $\tilde{\tau}_1^+ \tilde{\tau}_1^-$ pair production. Here, we see that it is quite easy to evade the ILC reach and still have a neutralino relic density consistent with (1.1). This is in contrast to prejudices from studies in the mid-1990s which favored the bulk annihilation region of
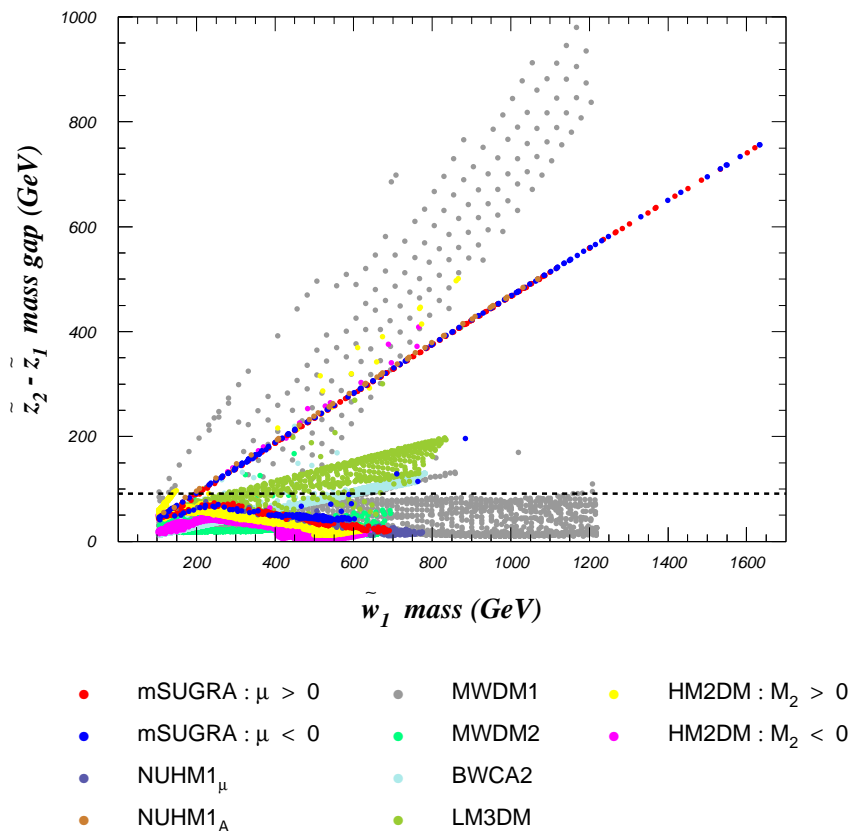
Figure 14: Predictions for $m_{\widetilde{W}_1}$ vs. $m_{\widetilde{Z}_2} - m_{\widetilde{Z}_1}$ from various models with $A_0 = 0$, $m_t = 171.4\,\text{GeV}$ and the sign of μ as in figure 12, but where the special parameter of non-universal mass models has been dialed to yield $\Omega_{\widetilde{Z}_1} h^2 \simeq 0.11$. We fix $\tan\beta = 10$ except for the mSUGRA model where we allow $\tan\beta = 10, 30, 45, 50, 52$ and 55. The dashed line denotes the point where $m_{\widetilde{Z}_2} - m_{\widetilde{Z}_1} = M_Z$, where the two-body spoiler decay mode $\widetilde{Z}_2 \to \widetilde{Z}_1 Z$ turns on.

mSUGRA, which then implied sparticle mass ought to be quite light, and likely accessible to LEP2 and ILC500 searches [9, 13]. The upper bands of mSUGRA model parameter points correspond to the HB/FP region, while the bands of points at low $m_{\tilde{\tau}_1}$ but high $m_{\widetilde{W}_1}$ correspond to the stau co-annihilation region in mSUGRA or in MWDM1 models.

4.2 Implications for $(g-2)_\mu$ and $BF(b \to s\gamma)$

The rare decay $b \to s\gamma$ has always been interesting for SUSY (as well as other new physics) studies, because the SM and the new physics contributions both occur at the one-loop order, and so are likely to be comparable if the particles in the new-physics loop have masses of about the weak scale. This is indeed the case for weak scale SUSY. The branching fraction $BF(b \to s\gamma)$ has been measured by the CLEO, Belle and BABAR collaborations; a

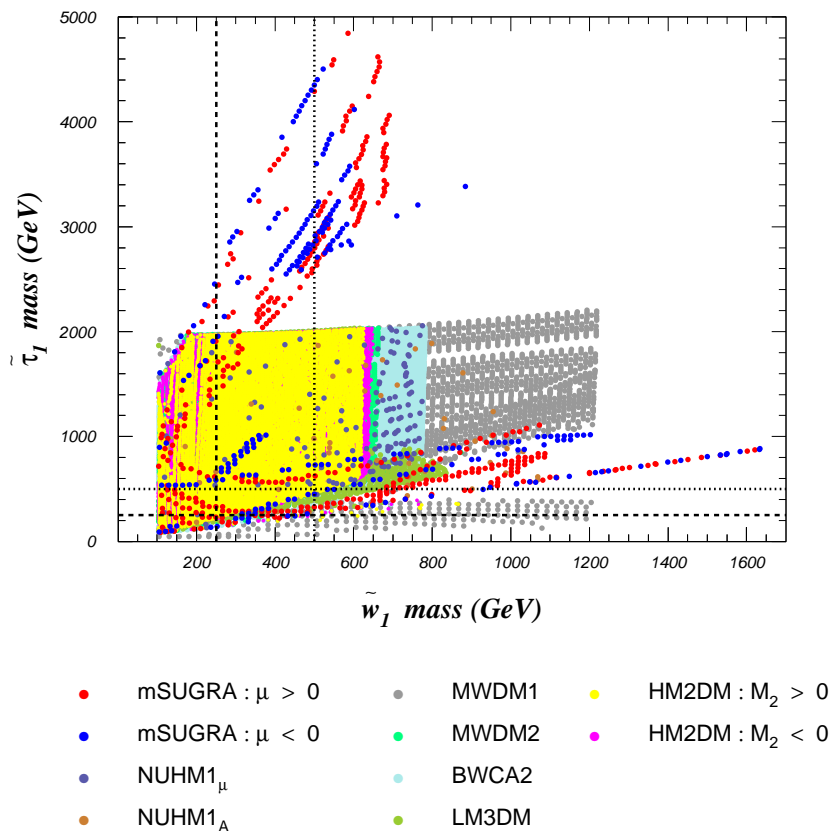**Figure 15:** Predictions for $m_{\widetilde{W}_1}$ $vs.$ $m_{\tilde{\tau}_1}$ from various models with $A_0 = 0$, $m_t = 171.4\,\text{GeV}$ and the sign of μ as in figure 12, but where the special parameter of non-universal mass models has been dialed to yield $\Omega_{\widetilde{Z}_1} h^2 \simeq 0.11$. We fix $\tan\beta = 10$ except for the mSUGRA model where we allow $\tan\beta = 10, 30, 45, 50, 52$ and 55. The dashed lines denote the approximate reach of ILC500, while dotted lines mark the approximate reach of ILC1000.

combined analysis [61] finds the branching fraction to be $BF(b \to s\gamma) = (3.55 \pm 0.26) \times 10^{-4}$, while a recent SM prediction [62] finds $BF(b \to s\gamma) = (3.15 \pm 0.23) \times 10^{-4}$. The theoretical error in the SUSY case may be somewhat larger. In figure 16, we show predictions for $BF(b \to s\gamma)$ in SUSY models where $\Omega_{\widetilde{Z}_1} h^2 \simeq 0.11$, against the value of $m_{\tilde{g}}$. We see that for models with low $m_{\tilde{g}}$, large deviations from the SM prediction are likely, although cases in agreement can be readily found. As $m_{\tilde{g}}$ increases, the SUSY loop contributions to $BF(b \to s\gamma)$ are suppressed. In the absence of an underlying theory of flavor, we should be careful in drawing strong inferences from this figure since even a small amount of flavor-violation in the textures of SSB parameters could significantly alter these predictions, with little impact on implications for direct searches at the LHC. That $BF(b \to s\gamma)$ has potentially larger SUSY contributions for mSUGRA models than in non-universal mass

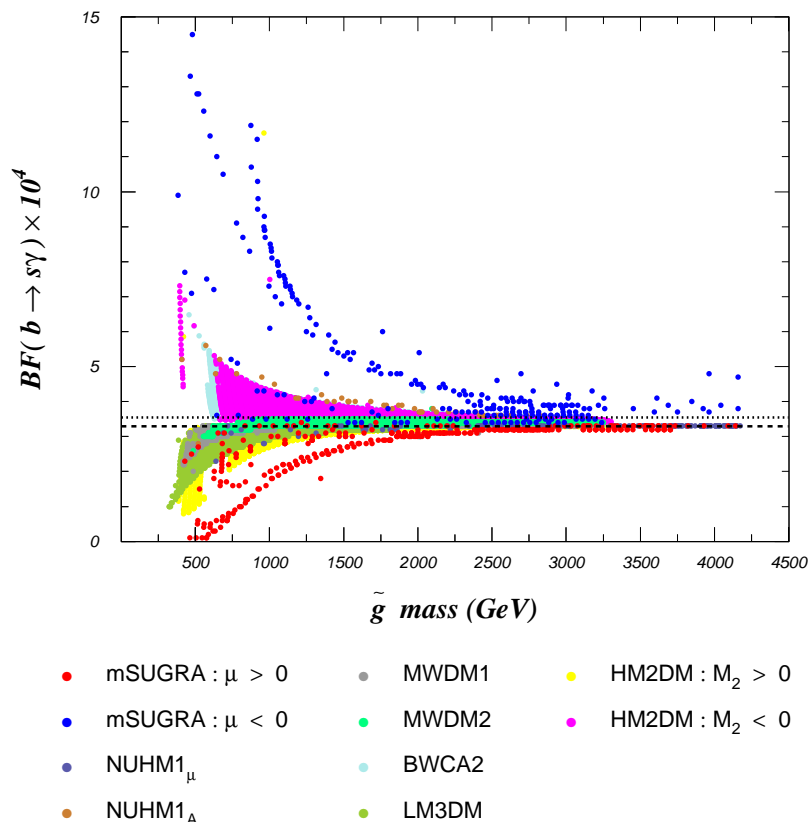**Figure 16:** Predictions for $BF(b \to s\gamma)$ *vs.* $m_{\tilde{g}}$ from various models with $A_0 = 0$, $m_t = 171.4\,\mathrm{GeV}$ and the sign of μ as in figure 12, but where the special parameter of non-universal mass models has been dialed to yield $\Omega_{\widetilde{Z}_1} h^2 \simeq 0.11$. We fix $\tan\beta = 10$ except for the mSUGRA model where we allow $\tan\beta = 10$, 30, 45, 50, 52 and 55. The dotted line denotes the central value of the combined experimental measurements, while the dashed line denotes the corresponding SM prediction. The SUSY contribution to the branching fraction is sensitive to $\tan\beta$ which is varied for the scans of the mSUGRA model, but fixed at $\tan\beta = 10$ for the scans in the case of non-universal mass models.

models is, of course, an artifact of our scans: for the mSUGRA model we scan large values of $\tan\beta$ while we fix $\tan\beta = 10$ for models with non-universal masses.

Recent measurements of the muon anomalous magnetic moment show an apparent deviation from SM predictions. Combining QED, electroweak, hadronic (using $e^+ e^- \to$ hadrons to evaluate hadronic loop contributions) and light-by-light contributions, and comparing against measurements from E821 at BNL, a *positive* deviation in $a_\mu \equiv \frac{(g-2)_\mu}{2}$ of

$$\Delta a_\mu = a_\mu^{\mathrm{exp}} - a_\mu^{\mathrm{SM}} = 22(10) \times 10^{-10} \tag{4.1}$$

is reported in the Particle Data Book [37], i.e. a 2.2σ effect.[6]

One-loop diagrams with $\widetilde{W}_i - \tilde{\nu}_\mu$ and $\widetilde{Z}_i - \tilde{\mu}_{1,2}$ in the loop would give supersymmetric contributions to a_μ, perhaps accounting for the (rather weak, yet persistent) discrepancy with the SM. In figure 17, we show $\Delta a_\mu^{\text{SUSY}}$ versus $m_{\tilde{\mu}_L}$. The dashed line indicates the central value of the experiment/theory discrepancy as presented by the Particle Data Group. We see that a variety of models are able to account for the discrepancy *as long as* $m_{\tilde{\mu}_L} \lesssim 1 - 1.5\,\text{TeV}$ for mSUGRA, but only about $500\,\text{GeV}$ in the case of models with non-universal mass parameters. This is partly a consequence of the fact that in mSUGRA our scans include large values of $\tan\beta$ in mSUGRA but are limited to $\tan\beta = 10$ for non-universal models. Since $\Delta a_\mu^{\text{SUSY}} \propto \tan\beta$, had we allowed larger values of $\tan\beta$ in our scans of models with non-universality, then the Δa_μ projections would increase beyond those plotted here, and consistency with the present central value would be possible for values of second generation slepton masses beyond the reach of a $1\,\text{TeV}$ ILC.

4.3 Implications for direct detection of dark matter

In figure 18, we show the spin-independent neutralino-proton scattering cross section, calculated with IsaReS program [64] from the IsaTools package, versus $m_{\widetilde{Z}_1}$. A significant uncertainty in the cross section comes from the value of the pion-nucleon Σ-term [65]. In this plot we assumed $\Sigma = 45\,\text{MeV}$, but larger values can increase our predictions by factor of about three. This plot is an update of similar results presented in ref. [30] in that it includes additional models. We also show the current limit established by the Xenon-10 collaboration [58] (solid line), along with the projected reaches for the SuperCDMS (25 kg) [66] (dashed line), LUX 300 kg [67](dot-dashed line) and Xenon-1 ton [68] (dotted line) experiments. The reach contours have been generated assuming a standard local density and velocity profile.

We see two distinct classes of models. In the first class, the neutralino-nucleon cross section falls off with $m_{\widetilde{Z}_1}$, while in the second class – models with a well-tempered neutralino with significant higgsino component – this cross section asymptotes to about 10^{-8} pb, within the reach of the next generation of detectors such as LUX-300 kg, Xenon-100 or super-CDMS. It is important to realize that this second class includes *several* of the specific models that we have considered where agreement with (1.1) is obtained via a significant higgsino component in the $\widetilde{Z}_1$ so that we have either mixed higgsino DM or mixed wino-bino-higgsino DM. This higgsino component then leads to a large cross section for $\widetilde{Z}_1 p$ scattering via diagrams involving h and/or H exchanges, where the Higgs bosons couple to the proton via both its quark and its gluon content. The neutralino annihilation rate in the early universe generally falls off with increasing $m_{\widetilde{Z}_1}$, so that for heavier neutralinos, a larger higgsino content is necessary to maintain the relic density at its observed value: it is precisely this increased higgsino-content that maintains the direct-detection cross section around 10^{-8} pb even for large values of $m_{\widetilde{Z}_1}$ in the upper branch of the figure. There are, however, many models where accord with the observed CDM relic density is obtained

---

[6]More recent analyses [63] report a larger discrepancy if only electron-positron data are used for the evaluation of the hadronic vacuum polarization contribution; the significance of the discrepancy is, however, reduced if tau decay data are used for this purpose.
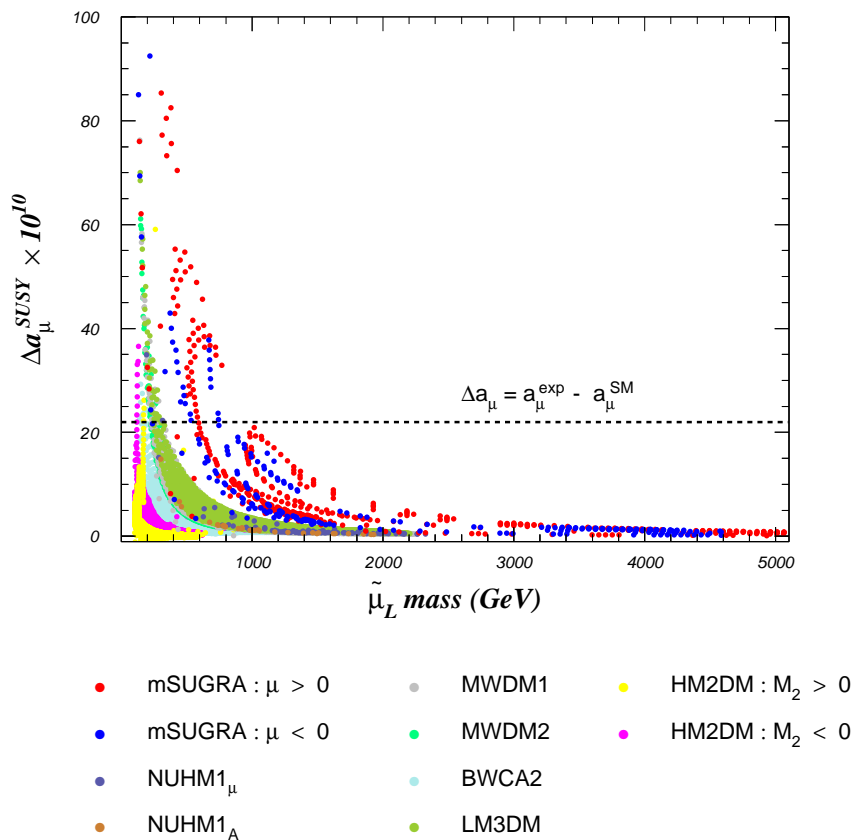
Figure 17: Predictions for $\Delta a_\mu^{\mathrm{SUSY}}$ $vs.$ $m_{\tilde{\mu}_L}$ from various models with $A_0 = 0$, $m_t = 171.4\,\mathrm{GeV}$ and the sign of μ as in figure 12, but where the special parameter of non-universal mass models has been dialed to yield $\Omega_{\widetilde{Z}_1} h^2 \simeq 0.11$. We fix $\tan\beta = 10$ except for the mSUGRA model where we allow $\tan\beta = 10, 30, 45, 50, 52$ and 55. The dashed line denotes the central value of the measured deviation from SM expectations as reported by the Particle Data Group, though some recent analyses would infer an even larger deviation as discussed in the text. Note that Δa_μ is sensitive to $\tan\beta$ which is varied for mSUGRA, but for scans of the non-universal mass models, is fixed to be 10.

by adjusting the *masses* to get either stau co-annihilation or bino-wino co-annihilation or Higgs funnel annihilation. In these cases of the bino-like LSP, the direct detection cross section falls with $m_{\widetilde{Z}_1}$ to below the sensitivity of even 1t noble element detectors for neutralino masses below about 400 GeV. There even are cases with $m_{\widetilde{Z}_1} \lesssim 100$ GeV where — due to interference between various contributing amplitudes [69, 30] (e.g. mSUGRA with $\mu < 0$) — the neutralino-nucleon scattering cross section drops to well below 10^{-10} pb, which is below the projected sensitivity of all proposed detectors to date. These same interference effects frequently lead to a reduced cross section in the BWCA2 case where we
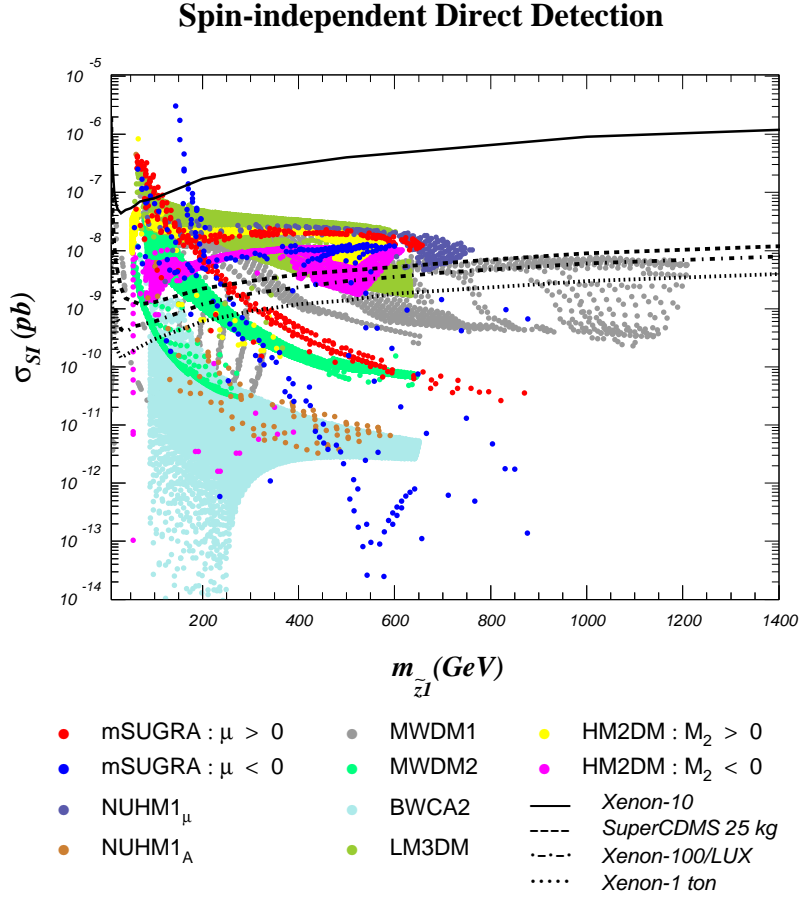
Spin-independent Direct Detection

Figure 18: Predictions for $\sigma_{\rm SI}(\widetilde{Z}_1 p)$ *vs.* $m_{\widetilde{Z}_1}$, generally regarded as the figure of merit for direct detection experiments, in various models with $A_0 = 0$, $m_t = 171.4\,{\rm GeV}$ and the sign of μ as in figure 12, but where the special parameter of non-universal mass models has been dialed to yield $\Omega_{\widetilde{Z}_1} h^2 \simeq 0.11$. We fix $\tan\beta = 10$ except for the mSUGRA model where we allow $\tan\beta = 10$, 30, 45, 50, 52 and 55. We also show the projected reach of selected direct detection experiments.

also take $\mu < 0$, the sign favored by the value of Δa_μ.

The neutralino may also scatter inside a detector via its spin-dependent coupling to the nucleon due to its couplings to the Z or to squarks. In figure 19 we show how this spin-dependent cross section is expected to scale with the corresponding spin-independent cross section in the various models that we have considered. It is striking to see that while the spin-dependent cross section in relic-density-consistent models may be as low as 10^{-8} pb, in well-tempered neutralino models where agreement with the relic density is obtained by adjusting the higgsino content of $\widetilde{Z}_1$ this cross section is always larger than 10^{-5} pb well above the projected sensitivity, $\sigma_{\rm SD}(\widetilde{Z}_1 p) \gtrsim 4 \times 10^{-7}$ pb, of the proposed COUPP experiment with a target mass of 1t [70]. This is of course, because higgsinos have a large coupling to the Z-boson. We note that there may be an observable signal via spin-
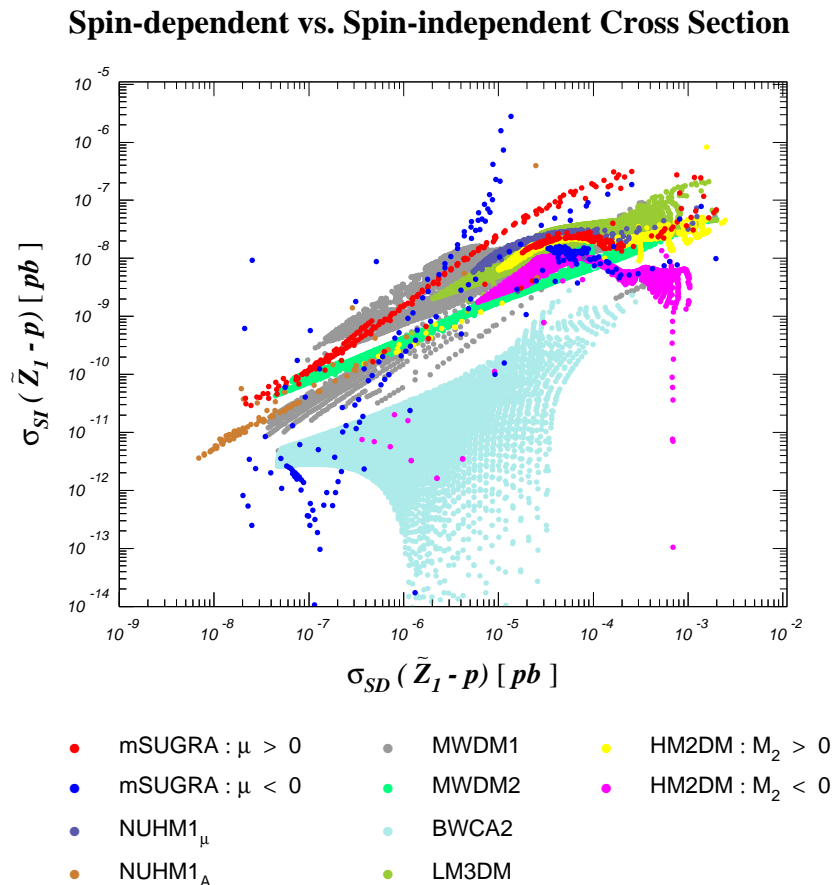
Spin-dependent vs. Spin-independent Cross Section

Figure 19: Predictions for $\sigma_{\rm SD}(\widetilde{Z}_1 p)$ *vs.* $\sigma_{\rm SI}(\widetilde{Z}_1 p)$ in various models with $A_0 = 0$, $m_t = 171.4\,{\rm GeV}$ and the sign of μ as in figure 12, but where the special parameter of non-universal mass models has been dialed to yield $\Omega_{\widetilde{Z}_1} h^2 \simeq 0.11$. We fix $\tan\beta = 10$ except for the mSUGRA model where we allow $\tan\beta = 10, 30, 45, 50, 52$ and 55.

dependent couplings even for cases where the prospects for direct detection via the spin-independent neutralino interaction appear to be hopeless. We also remark that the 50 kg prototype of the COUPP detector is projected to have a sensitivity $\sigma_{\rm SD}(\widetilde{Z}_1 p) \sim 4 \times 10^{-4}$ pb.

4.4 Implications for indirect detection of dark matter: neutrino telescopes

In figure 20, we show the flux of muons with $E_\mu > 50\,{\rm GeV}$ which is expected from neutralino capture by the sun, with subsequent neutralino annihilation in the solar core to ν_μ states (for some recent work, see ref. [72]). To calculate these and subsequent indirect dark matter detection rates, we use the DarkSUSY [73] - Isajet interface. The flux of high energy ν_μ from neutralino annihilation in the solar core depends on both the neutralino capture cross section as well as on the neutralino annihilation cross section. The capture rate mainly depends on the *spin-dependent* neutralino-nucleon cross section, the main contribution to

which comes from Z-exchange processes that are enhanced if the neutralino has a significant higgsino content. Note that it is easily possible to have a large spin-independent neutralino-nucleon scattering cross section, and yet a small spin-dependent cross section, leading to undetectable rates in the IceCube experiment This is exemplified in figure 20, we *again* find that the well-tempered neutralino models aggregate around an asymptotic regime of $\sim 10 - 100$ events/km^2/yr. The approximate reach of IceCube for $E_\mu > 50\,\mathrm{GeV}$ is around the 40 events/km^2/yr [74], so again many of the models with mixed gaugino/higgsino dark matter stand a good chance of indirect detection via neutrino telescopes, whereas models where (1.1) is satisfied in other ways fall below the detectable level. We remark though that if $m_{\widetilde{Z}_1} \sim 100\,\mathrm{GeV}$, even the signal from BWCA2 may be in the detectable range. We mention that projections for IceCube, unlike those for indirect detection from neutralino annihilation to anti-matter or gamma rays (discussed next), are only slightly sensitive to the DM halo profile.

4.5 Implications for indirect detection of dark matter from halo annihilations

An alternative method for indirect detection of dark matter is to search for the debris resulting from dark matter annihilation in the galactic halo. One promising method is to search for GeV-scale γ-rays, which could come directly from $\widetilde{Z}_1\widetilde{Z}_1 \to \gamma\gamma$ via a box and triangle diagrams, or via $\widetilde{Z}_1\widetilde{Z}_1 \to q\bar{q}$, where hadronization and decay lead to gamma rays via the $q \to \pi^0 \to \gamma$ chain. The direct process occurs at low rates, but would have a characteristic signal at the source with $E_\gamma \simeq m_{\widetilde{Z}_1}$, whereas gamma rays coming from quark hadronization should be more abundant, but will yield a continuum distribution in E_γ with a cut-off at $m_{\widetilde{Z}_1}$.

Since γ-rays from neutralino annihilation should propagate undeflected through the galaxy, a good place to look is the galactic center, where the DM density is expected to be high. In figure 21, we show the flux of γ-rays coming from the direction of the galactic center with $E_\gamma > 1\,\mathrm{GeV}$, in units of events/cm^2/s. The result is very sensitive to the choice of the galactic dark matter density profile, as well as to (unknown) details of how clumpy the halo distribution is. We show results for the Adiabatically Contracted N03 halo profile [75], where the deepening of gravitational potential wells caused by baryon in-fall leads to a higher DM concentration in the center of the Milky Way, and a concomitantly larger gamma ray flux. Other halo distributions, such as the Burkert profile [76], where the central DM halo cusp is smoothed out by significant re-heating, predict gamma ray fluxes that may be *four orders of magnitude smaller*! The reach of the GLAST satellite experiment is indicated by the dashed line [77]. The important point is that models with large s-wave neutralino annihilation cross sections cluster around an asymptotic level of $\sim 10^{-7}$/cm^2/s, while models which rely on co-annihilation such as BWCA or MWDM2 predict much lower gamma ray fluxes. A notable difference between signals from halo annihilation versus signals from direct and neutrino detection is that the halo annihilation signals can be enhanced by moving $2m_{\widetilde{Z}_1}$ onto the A-resonance [43]: if neutralinos have enhanced annihilation through the A-funnel in the early universe, then they can also readily annihilate through the A-funnel in the galactic halo (this does not hold true for the h and H resonances, which are dominantly p-wave, or the Z pole, which is not resonance
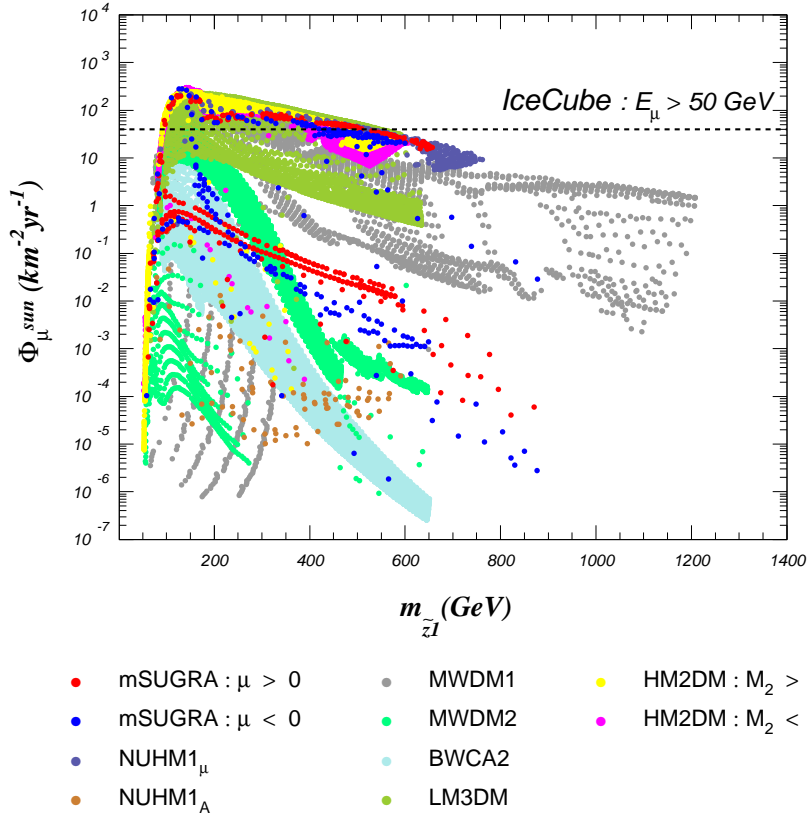
Neutrino Detection

Figure 20: Predictions for muon flux with $E_\mu > 50\,\text{GeV}$ Φ_μ *vs.* $m_{\widetilde{Z}_1}$ from various models with $A_0 = 0$, $m_t = 171.4\,\text{GeV}$ and the sign of μ as in figure 12, but where the special parameter of non-universal mass models has been dialed to yield $\Omega_{\widetilde{Z}_1} h^2 \simeq 0.11$. We fix $\tan\beta = 10$ except for the mSUGRA model where we allow $\tan\beta = 10$, 30, 45, 50, 52 and 55. The region above the dashed line denotes the approximate reach of the IceCube neutrino telescope.

enhanced [5]). In the case of γ-ray signals, we see the orange dots from NUHM1$_A$ model now populate higher rate levels than the BWCA and MWDM2 cases, whereas for direct and ν_μ signals in figures 18 and 20, the NUHM1$_A$ signal was comparable to or even lower than the BWCA and MWDM2 models.

Another characteristic signature of DM halo annihilations is the detection of large fluxes of anti-particles such as $\bar{p}$s, e^+s or anti-deuterons $\bar{D}$. For positrons and antiprotons, we evaluate the averaged differential antiparticle flux in a projected energy bin centered at a kinetic energy of $20\,\text{GeV}$, where we expect an optimal statistics and signal-to-background ratio at space-borne antiparticle detectors [78, 79]. We take the experimental sensitivity to be that of the Pamela experiment after three years of data-taking as our benchmark. For $\bar{D}$s, we evaluate the average differential anti-deuteron flux in the $0.1 < T_{\bar{D}} < 0.25\,\text{GeV}$
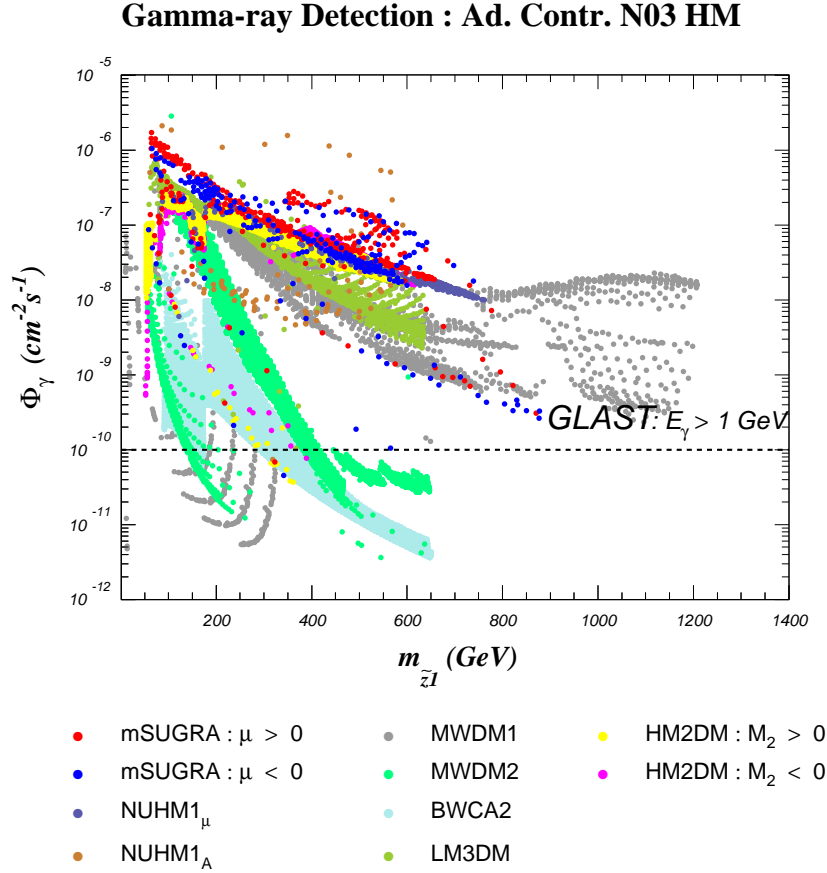
Gamma-ray Detection : Ad. Contr. N03 HM

Figure 21: Predictions for gamma ray flux with $E_\gamma > 1\,\mathrm{GeV}$ from various models with $A_0 = 0$, $m_t = 171.4\,\mathrm{GeV}$ and the sign of μ as in figure 12, but where the special parameter of non-universal mass models has been dialed to yield $\Omega_{\widetilde{Z}_1} h^2 \simeq 0.11$. We fix $\tan\beta = 10$ except for the mSUGRA model where we allow $\tan\beta = 10, 30, 45, 50, 52$ and 55. We adopt the Adiabatically Contracted N03 DM halo profile. The region above the dashed line denotes the approximate reach of the GLAST experiment. The flux predicted from less cusped halo profiles may be down by as much as four orders of magnitude.

range, where $T_{\bar{D}}$ stands for the anti-deuteron kinetic energy per nucleon, and compare it to the estimated GAPS sensitivity for an ultra-long duration balloon-borne experiment [80] (see ref. [81] for an updated discussion of the role of antideuteron searches in DM indirect detection).

In figure 22 we show the flux of $\bar{p}$s assuming the Adiabatically Contracted N03 halo profile; results from using the Burkert profile yield results typically a factor of 10-20 below these. The models with mixed higgsino dark matter cluster at high levels of around $\sim 10^{-8}$ events/GeV/cm^2/s/sr while the A-funnel annihilation case of NUHM1$_A$ populates the $10^{-9} - 10^{-7}$ events/GeV/cm^2/s/sr range. The co-annihilation cases BWCA and MWDM2
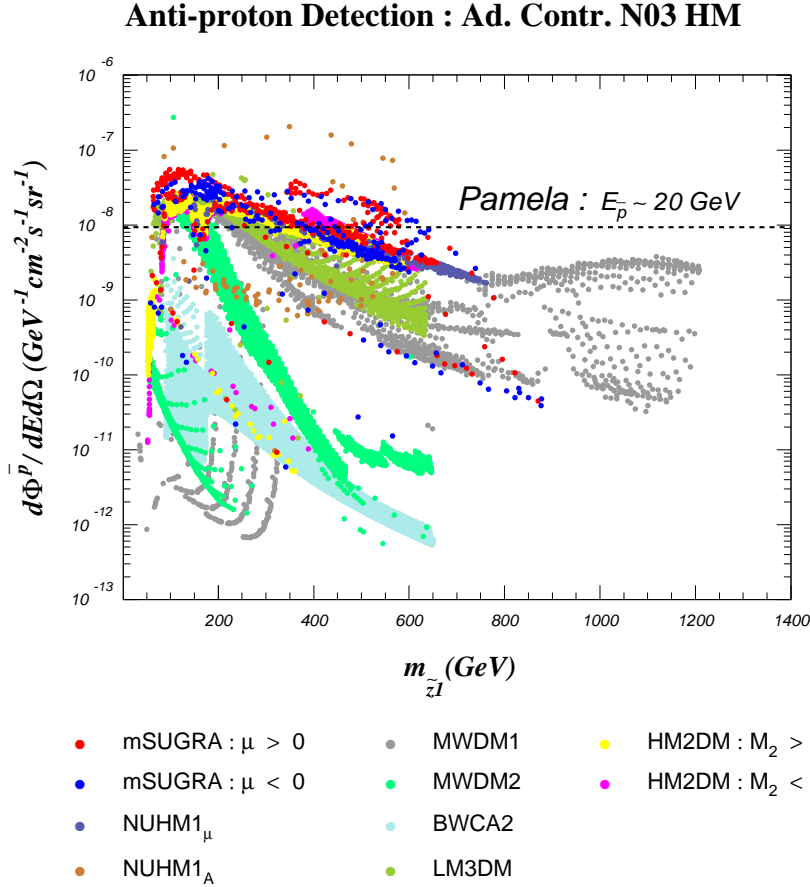
Anti-proton Detection : Ad. Contr. N03 HM

Figure 22: Predictions for anti-proton flux from various models with $A_0 = 0$, $m_t = 171.4$ GeV and the sign of μ as in figure 12, but where the special parameter of non-universal mass models has been dialed to yield $\Omega_{\widetilde{Z}_1} h^2 \simeq 0.11$. We fix $\tan\beta = 10$ except for the mSUGRA model where we allow $\tan\beta = 10, 30, 45, 50, 52$ and 55. We adopt the Adiabatically Contracted N03 DM halo profile. The region above the dashed line denotes the approximate reach of the PAMELA experiment.

and stau-co-annihilation in mSUGRA lie at much lower levels.

In figure 23 we show the flux of e^+s using the Adiabatically Contracted N03 halo profile; results from using the Burkert profile yield results about a factor of 3-5 lower.[7] Our projections are not optimistic. The models with mixed higgsino dark matter cluster at the $\sim 10^{-9}$ events/GeV/cm^2/s/sr level, which may be just below the Pamela reach [82]. The A-funnel annihilation case of NUHM1$_A$ populates the $10^{-10} - 10^{-8}$ events/GeV/cm^2/s/sr range. The co-annihilation cases BWCA and MWDM2 and stau-coannihilation in mSUGRA are

---

[7]To reach earth before losing too much energy and annihilating, the positrons must originate from annihilation much closer to earth than for $\bar{p}$s or γs; thus, predictions for their flux are less sensitive than those for anti-protons and gamma rays to the choice of halo profile. Different halo distributions mainly differ on the DM density near the galactic center, but agree on the local DM density.
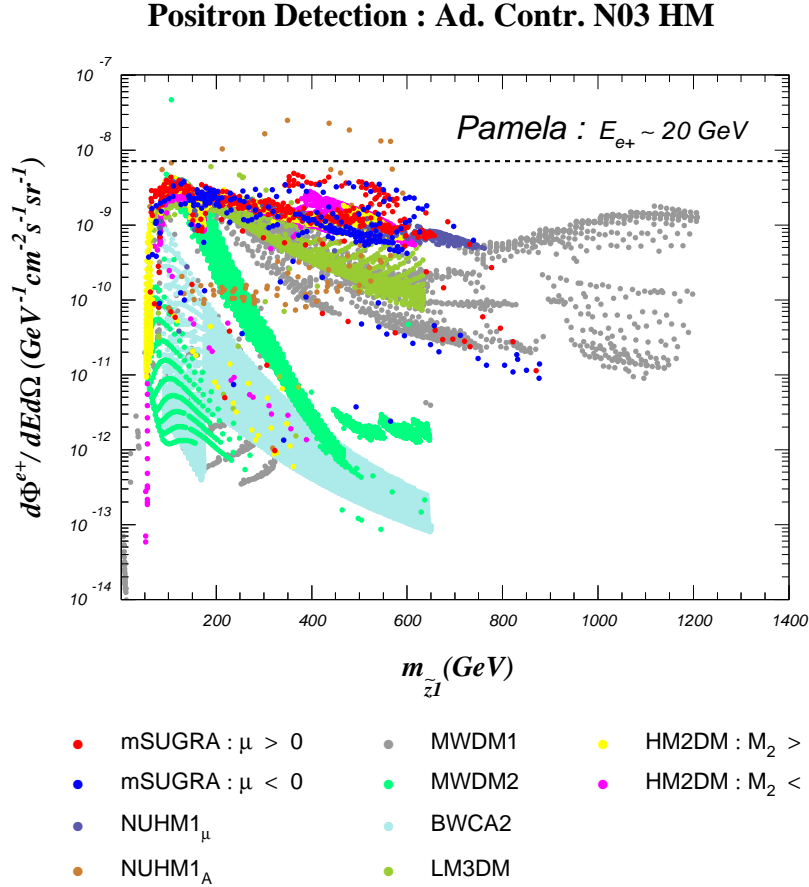
Positron Detection : Ad. Contr. N03 HM

Figure 23: Predictions for positron flux from various models with $A_0 = 0$, $m_t = 171.4\,\text{GeV}$ and the sign of μ as in figure 12, but where the special parameter of non-universal mass models has been dialed to yield $\Omega_{\widetilde{Z}_1} h^2 \simeq 0.11$. We fix $\tan\beta = 10$ except for the mSUGRA model where we allow $\tan\beta = 10$, 30, 45, 50, 52 and 55. We adopt the Adiabatically Contracted N03 DM halo profile. The region above the dashed line denotes the approximate reach of the PAMELA experiment.

again at much lower levels.

In figure 24, we show the predicted flux of anti-deuterons expected in a kinetic energy range $T_{\bar{D}} = 0.1 - 0.25\,\text{GeV}$ using the Adiabatically Contracted N03 halo profile, suitable for detection by the proposed GAPS experiment. Results using the Burkert profile tend to be a factor of 10-20 lower, about the same as for anti-protons. Models with mixed higgsino dark matter populate the 10^{-11} events/GeV/cm^2/s/sr level, and should be accessible to GAPS via the long duration balloon flight. The NUHM1$_A$ model populates points just below to just above the GAPS sensitivity level, while the co-annihilation models give results which are generally beyond reach of any foreseeable experiment.

In drawing inferences for prospects for indirect detection from the scans of non-universal mass models discussed in this section, we should keep in mind that we have
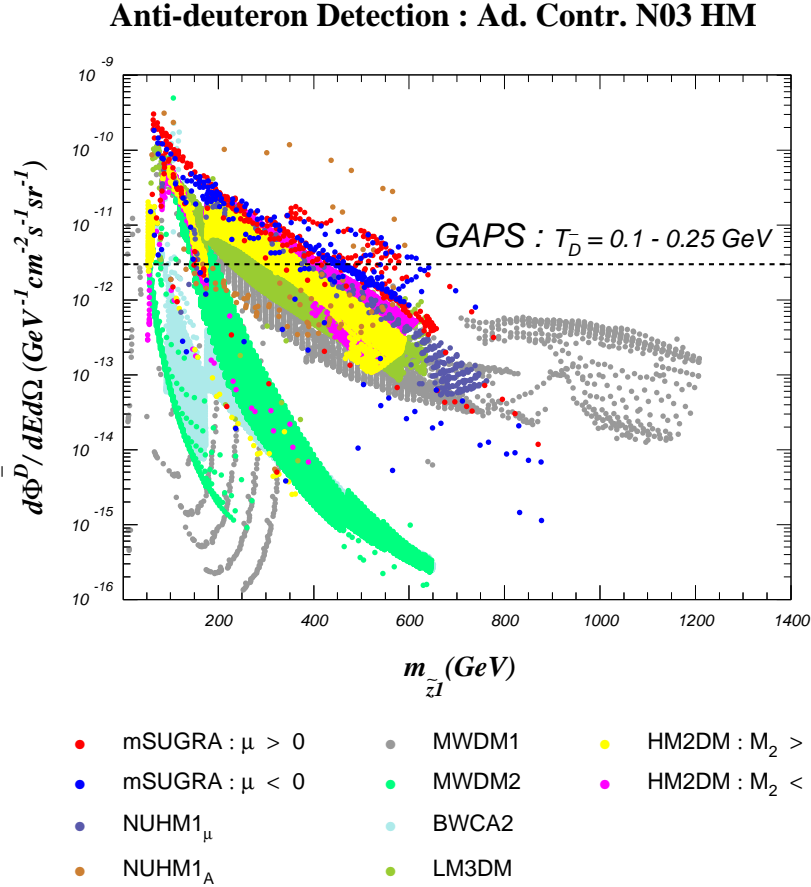
Anti-deuteron Detection : Ad. Contr. N03 HM

Figure 24: Predictions for anti-deuteron flux from various models with $A_0 = 0$, $m_t = 171.4\,\text{GeV}$ and the sign of μ as in figure 12, but where the special parameter of non-universal models has been dialed to yield $\Omega_{\widetilde{Z}_1} h^2 \simeq 0.11$. We fix $\tan\beta = 10$ except for the mSUGRA model where we allow $\tan\beta = 10, 30, 45, 50, 52$ and 55. We adopt the Adiabatically Contracted N03 DM halo profile. The region above the dashed line denotes the approximate reach of the GAPS experiment.

shown results for just the Adiabatically Contracted N03 halo profile (for detailed comparison of halo profiles, see e.g. ref. [22] and [43]) and fixed $\tan\beta = 10$. Typically, we have found that the indirect searches are most sensitive to the higgsino component in the $\widetilde{Z}_1$. It is important to note that direct detection and indirect detection via halo annihilation both grow as $\tan\beta$ is increased.

5. Summary and concluding remarks

If the observed cold dark matter [1] is interpreted as thermal relic neutralinos of R-parity conserving supersymmetric models, then the determination of the CDM relic density (1.1) provides a very strong constraint, effectively reducing the dimension of model parameter

space by one unit. It is then reasonable to ask how this relic density measurement constrains on what other experiments searching for SUSY might or might not observe.

Indeed many groups have analyzed the implications of the measured value of the CDM relic density for SUSY signals at the LHC within the mSUGRA framework. Toward the end of section 1, we enumerated several broad conclusions that were drawn from these studies. In order to test the robustness of these conclusions, it is necessary to examine how these are affected if we relax the *untested* universality assumptions that are the hallmark of the mSUGRA framework. Motivated by this, as well as by the fact that most of the relic-density-allowed range of parameters lies on the periphery of mSUGRA parameter space, we have examined a variety of models where universality of scalar or gaugino SSB mass parameters is relaxed via the introduction of just one additional parameter that is then adjusted so that the thermal relic density of neutralinos matches (1.1), by adjusting either the neutralino composition or its mass. In section 3, we show explicit examples of these various models that lead to broadly similar sparticle mass spectra, and compare and contrast the features of the different models with the paradigm mSUGRA framework, and with one another.

Prior to the analyses of non-universal models, there were several prejudices inferred from studies based on mSUGRA, and frequently held to be true, including:

1. The relic-density-consistent bulk region implies a variety of light sparticles accessible at the LHC, and possibly the ILC;

2. The Higgs-funnel region only occurs at large $\tan\beta$, where down-type Yukawa couplings are necessarily large, so that sparticle decay cascades are modified, with concomitant effects on collider signatures;

3. The higgsino-content of the neutralino LSP can only be large enough to get agreement with (1.1) only if scalars are essentially decoupled at the LHC;

4. The lighter $\tilde{b}$-squark is dominantly $\tilde{b}_L$ while the lighter stau is dominantly $\tilde{\tau}_R$.

We have seen that even in relatively innocuous one-parameter extensions of mSUGRA each of these conclusions is false. For instance, the HS model allows rapid neutralino annihilation via light $\tilde{u}_R/\tilde{c}_R$ with other sparticles much heavier, or via $\tilde{\tau}_1$ which is dominantly $\tilde{\tau}_L$, the Higgs-funnel occurs for any value of $\tan\beta$ in the NUHM1 model, and we can have MHDM for rather small scalar masses, also in the NUHM1 model. While it is definitely worthwhile to correlate the implications of one observation with what might and might not be seen in other experiments, our analysis highlights the fact that such inferences are frequently dependent on underlying assumptions. In particular, we caution against drawing broad conclusions about what is or is not likely at the LHC based upon studies of just the mSUGRA model.

In section 4 we have performed scans over the parameter space of the mSUGRA as well as over eight of its one-parameter extensions to abstract features common to relic-density-consistent models. We end by summarizing our broad conclusions based on these scans.

- In mSUGRA, a well-tempered neutralino LSP can only be obtained in the HB/FP region, where squark and slepton masses are far heavier than the lightest charginos, neutralinos and gluino. In non-universal models, we can easily have a well-tempered neutralino with $m_{\tilde{q}} \sim m_{\tilde{g}}$. Indeed except for the HB/FP region of mSUGRA, squark and gluino masses are typically comparable in relic-density-consistent models. In a similar vein, we also note that while Higgs-funnel enhancement is possible only for very large values of $\tan\beta$ in the mSUGRA framework, if we allow for non-universality of Higgs SSB parameters, we can have the Higgs funnel for any value of $\tan\beta$.

- In many relic-density-consistent models, the $\widetilde{Z}_2 - \widetilde{Z}_1$ mass gap is usually less than M_Z, so that two-body spoiler decays modes of $\widetilde{Z}_2$ are kinematically closed. This means that at least one dilepton mass edge (and perhaps more) is likely to be detectable at LHC. The location of the dilepton mass edge(s) is a rather clean signature of supersymmetric models, and often serves as the starting point for sparticle mass reconstruction.

- Most relic-density-consistent models should lead to observable signals at the LHC. In contrast, while models where accord with the observed relic density is obtained by tempering the higgsino-content of the neutralino will likely be accessible at a $1\,\mathrm{TeV}$ electron-positron collider, in other scenarios sparticles may simply be too heavy to be accessible.

- In well-tempered neutralino models, the mechanism that enhances annihilation in the early universe also tends to enhance the direct DM detection rate. In particular, models tempered via the higgsino content of the LSP typically have $\sigma_{\mathrm{SI}}(\widetilde{Z}_1 p) \sim 10^{-8}$ pb, which ought to be accessible to the next set of direct detection experiments, including LUX, Xenon-100, WARP, mini-CLEAN and SuperCDMS: see figure 18. These experiments may also provide a measure of the mass of the halo DM particle(s), assuming that it is not very heavy compared to the target nucleus [83].[8] If a signal is found in these direct detection experiments, it can be directly compared to expectations based on SUSY model parameters extracted in experiments at the LHC and especially the ILC to test whether thermally produced neutralinos indeed saturate the measured value of the cold DM density [84], or whether DM, like visible matter, turns out to have more than one component.

- Likewise, these models have elevated rates for indirect DM detection via neutrino telescopes. In this case, the flux of muon neutrinos tends to be above $\Phi_\mu \sim 10$ events/km^2/year for $E_\nu > 50\,\mathrm{GeV}$. In many such models, the signal should be accessible at the IceCube detector, as can be seen from figure 20.

- Finally, well-tempered neutralino models also have elevated rates for indirect DM searches via neutralino annihilation in the galactic halo into gamma rays and anti-matter, especially if the higgsino component is enhanced: see figure 21-24. These

---

[8]Direct detection experiments with different target nuclei ranging over a wide range of masses may thus provide clear evidence for multiple WIMP components in the galactic halo.

rates have large uncertainties associated with the presently unknown galactic dark matter density profile. But if a signal is found, it can be compared to expectations using model parameters extracted from LHC and ILC measurements, and the measured halo annihilation rate can be used to determine the DM halo profile [84].

Acknowledgments

References

[1] WMAP collaboration, D.N. Spergel et al., *Wilkinson Microwave Anisotropy Probe (WMAP) three year results: implications for cosmology*, Astrophys. J. Suppl. **170** (2007) 377 [astro-ph/0603449].

[2] H. Baer and X. Tata, *Weak scale supersymmetry: from superfields to scattering events*, Cambridge University Press, Cambridge U.K. (2006).

[3] M. Drees, R. Godbole and P. Roy, *Theory and phenomenology of sparticles*, World Scientific (2004);
P. Binétruy, *Supersymmetry*, Oxford University Press, Oxford U.K. (2006);
S.P. Martin, *A supersymmetry primer*, hep-ph/9709356.

[4] H. Goldberg, *Constraint on the photino mass from cosmology*, Phys. Rev. Lett. **50** (1983) 1419;
J.R. Ellis, J.S. Hagelin, D.V. Nanopoulos and M. Srednicki, *Search for supersymmetry at the $\bar{p}p$ collider*, Phys. Lett. **B 127** (1983) 233;
J.R. Ellis, J.S. Hagelin, D.V. Nanopoulos, K.A. Olive and M. Srednicki, *Supersymmetric relics from the Big Bang*, Nucl. Phys. **B 238** (1984) 453.

[5] For recent reviews, see e.g., G. Jungman, M. Kamionkowski and K. Griest, *Supersymmetric dark matter*, Phys. Rept. **267** (1996) 195 [hep-ph/9506380];
A.B. Lahanas, N.E. Mavromatos and D.V. Nanopoulos, *WMAPing the universe: supersymmetry, dark matter, dark energy, proton decay and collider physics*, Int. J. Mod. Phys. **D 12** (2003) 1529 [hep-ph/0308251];
M. Drees, *Supersymmetric dark matter 2004*, hep-ph/0410113;
K.A. Olive, *Astroparticle physics*, astro-ph/0503065.

[6] J.R. Ellis, K.A. Olive, Y. Santoso and V.C. Spanos, *Supersymmetric dark matter in light of WMAP*, Phys. Lett. **B 565** (2003) 176 [hep-ph/0303043];
H. Baer and C. Balázs, *χ^2 analysis of the minimal supergravity model including WMAP, $g(\mu) - 2$ and $b \to s\gamma$ constraints*, JCAP **05** (2003) 006 [hep-ph/0303114];
U. Chattopadhyay, A. Corsetti and P. Nath, *WMAP constraints, SUSY dark matter and implications for the direct detection of SUSY*, Phys. Rev. **D 68** (2003) 035005 [hep-ph/0303201];

A.B. Lahanas and D.V. Nanopoulos, *WMAPing out supersymmetric dark matter and phenomenology*, *Phys. Lett.* **B 568** (2003) 55 [hep-ph/0303130];

A. Djouadi, M. Drees and J.-L. Kneur, *Updated constraints on the minimal supergravity model*, *JHEP* **03** (2006) 033 [hep-ph/0602001].

[7] A.H. Chamseddine, R. Arnowitt and P. Nath, *Locally supersymmetric grand unification*, *Phys. Rev. Lett.* **49** (1982) 970;

R. Barbieri, S. Ferrara and C.A. Savoy, *Gauge models with spontaneously broken local supersymmetry*, *Phys. Lett.* **B 119** (1982) 343;

N. Ohta, *Grand unified theories based on local supersymmetry*, *Prog. Theor. Phys.* **70** (1983) 542;

L.J. Hall, J.D. Lykken and S. Weinberg, *Supergravity as the messenger of supersymmetry breaking*, *Phys. Rev.* **D 27** (1983) 2359;

H.P. Nilles, *Supersymmetry, Supergravity and Particle Physics*, *Phys. Rept.* **110** (1984) 1;

P. Nath, *Twenty years of SUGRA*, hep-ph/0307123.

[8] K. Ichikawa, M. Kawasaki, K. Nakayama, M. Senami and F. Takahashi, *Increasing effective number of neutrinos by decaying particles*, *JCAP* **05** (2007) 008 [hep-ph/0703034].

[9] H. Baer and M. Brhlik, *Cosmological relic density from minimal supergravity with implications for collider physics*, *Phys. Rev.* **D 53** (1996) 597 [hep-ph/9508321];

V.D. Barger and C. Kao, *Relic density of neutralino dark matter in supergravity models*, *Phys. Rev.* **D 57** (1998) 3131 [hep-ph/9704403].

[10] J.R. Ellis, T. Falk and K.A. Olive, *Neutralino stau coannihilation and the cosmological upper limit on the mass of the lightest supersymmetric particle*, *Phys. Lett.* **B 444** (1998) 367 [hep-ph/9810360];

J. Ellis, T. Falk, K. Olive and M. Srednicki, *Calculations of neutralino-stau coannihilation channels and the cosmologically relevant region of MSSM parameter space*, *Astropart. Phys.* **13** (2000) 181 [*Erratum ibid.* **15** (2001) 413] [hep-ph/9905481];

M.E. Gómez, G. Lazarides and C. Pallis, *Supersymmetric cold dark matter with Yukawa unification*, *Phys. Rev.* **D 61** (2000) 123512 [hep-ph/9907261]; *Yukawa unification, $b \to s\gamma$ and bino stau coannihilation*, *Phys. Lett.* **B 487** (2000) 313 [hep-ph/0004028];

A.B. Lahanas, D.V. Nanopoulos and V.C. Spanos, *Neutralino relic density in a universe with non-vanishing cosmological constant*, *Phys. Rev.* **D 62** (2000) 023515 [hep-ph/9909497];

R. Arnowitt, B. Dutta and Y. Santoso, *Coannihilation effects in supergravity and D-brane models*, *Nucl. Phys.* **B 606** (2001) 59 [hep-ph/0102181].

[11] K.L. Chan, U. Chattopadhyay and P. Nath, *Naturalness, weak scale supersymmetry and the prospect for the observation of supersymmetry at the Tevatron and at the LHC*, *Phys. Rev.* **D 58** (1998) 096004 [hep-ph/9710473];

J.L. Feng, K.T. Matchev and T. Moroi, *Multi-TeV scalars are natural in minimal supergravity*, *Phys. Rev. Lett.* **84** (2000) 2322 [hep-ph/9908309]; *Focus points and naturalness in supersymmetry*, *Phys. Rev.* **D 61** (2000) 075005 [hep-ph/9909334];

see also, H. Baer, C.-H. Chen, F. Paige and X. Tata, *Signals for minimal supergravity at the CERN large hadron collider: multi-jet plus missing energy channel*, *Phys. Rev.* **D 52** (1995) 2746 [hep-ph/9503271]; *Signals for minimal supergravity at the CERN Large Hadron Collider II: multilepton channels*, *Phys. Rev.* **D 53** (1996) 6241 [hep-ph/9512383];

H. Baer, C.-H. Chen, M. Drees, F. Paige and X. Tata, *Probing minimal supergravity at the CERN LHC for large $\tan\beta$*, *Phys. Rev.* **D 59** (1999) 055014 [hep-ph/9809223];

for a model-independent approach, see H. Baer, T. Krupovnickas, S. Profumo and P. Ullio, *Model independent approach to focus point supersymmetry: from dark matter to collider searches*, *JHEP* **10** (2005) 020 [hep-ph/0507282].

[12] M. Drees and M.M. Nojiri, *The Neutralino relic density in minimal* $N = 1$ *supergravity*, *Phys. Rev.* **D 47** (1993) 376 [hep-ph/9207234]; *Neutralino dark matter in minimal supergravity: direct detection vs. collider searches*, *Phys. Rev.* **D 57** (1998) 567 [hep-ph/9706509];
H. Baer et al., *Yukawa unified supersymmetric* SO(10) *model: cosmology, rare decays and collider searches*, *Phys. Rev.* **D 63** (2001) 015007 [hep-ph/0005027];
J.R. Ellis, T. Falk, G. Ganis, K.A. Olive and M. Srednicki, *The CMSSM parameter space at large* $\tan\beta$, *Phys. Lett.* **B 510** (2001) 236 [hep-ph/0102098];
L. Roszkowski, R. Ruiz de Austri and T. Nihei, *New cosmological and experimental constraints on the CMSSM*, *JHEP* **08** (2001) 024 [hep-ph/0106334];
A. Djouadi, M. Drees and J.L. Kneur, *Constraints on the minimal supergravity model and prospects for SUSY particle production at future linear* e^+e^- *colliders*, *JHEP* **08** (2001) 055 [hep-ph/0107316];
A.B. Lahanas and V.C. Spanos, *Implications of the pseudo-scalar Higgs boson in determining the neutralino dark matter*, *Eur. Phys. J.* **C 23** (2002) 185 [hep-ph/0106345].

[13] P. Nath and R. Arnowitt, *Predictions in* SU(5) *supergravity grand unification with proton stability and relic density constraints*, *Phys. Rev. Lett.* **70** (1993) 3696 [hep-ph/9302318];
A. Djouadi, M. Drees and J.-L. Kneur, *Neutralino dark matter in mSUGRA: reopening the light Higgs pole window*, *Phys. Lett.* **B 624** (2005) 60 [hep-ph/0504090].

[14] C. Böhm, A. Djouadi and M. Drees, *Light scalar top quarks and supersymmetric dark matter*, *Phys. Rev.* **D 62** (2000) 035012 [hep-ph/9911496];
J.R. Ellis, K.A. Olive and Y. Santoso, *Calculations of neutralino-stop coannihilation in the CMSSM*, *Astropart. Phys.* **18** (2003) 395 [hep-ph/0112113];
J. Edsjö, M. Schelke, P. Ullio and P. Gondolo, *Accurate relic densities with neutralino, chargino and sfermion coannihilations in mSUGRA*, *JCAP* **04** (2003) 001 [hep-ph/0301106].

[15] S. Dimopoulos and H. Georgi, *Softly broken supersymmetry and* SU(5), *Nucl. Phys.* **B 193** (1981) 150;
for a detailed phenomenological analysis, see F. Gabbiani, E. Gabrielli, A. Masiero and L. Silvestrini, *A complete analysis of FCNC and CP constraints in general SUSY extensions of the standard model*, *Nucl. Phys.* **B 477** (1996) 321 [hep-ph/9604387].

[16] For an update, see S. Kraml, *CP violation in SUSY*, arXiv:0710.5117.

[17] See e.g. J. Feng, A. Rajaraman and F. Takayama, *SuperWIMP dark matter signals from the early universe*, *Phys. Rev.* **D 68** (2003) 063504 [hep-ph/0306024].

[18] H. Baer, M.A. Diaz, P. Quintana and X. Tata, *Impact of physical principles at very high energy scales on the superparticle mass spectrum*, *JHEP* **04** (2000) 016 [hep-ph/0002245].

[19] A. Datta, A. Datta, M. Drees and D.P. Roy, *Effects of* SO(10) *D-terms on SUSY signals at the Tevatron*, *Phys. Rev.* **D 61** (2000) 055003 [hep-ph/9907444].

[20] H. Baer, A. Belyaev, T. Krupovnickas and A. Mustafayev, *SUSY normal scalar mass hierarchy reconciles* $(g - 2)(\mu)$, $b \to s\gamma$ *and relic density*, *JHEP* **06** (2004) 044 [hep-ph/0403214];
S.F. King and J.P. Roberts, *Universality of k-string tensions from holography and the lattice*, *JHEP* **09** (2006) 036.

[21] H. Baer, A. Mustafayev, S. Profumo, A. Belyaev and X. Tata, *Neutralino cold dark matter in a one parameter extension of the minimal supergravity model*, *Phys. Rev.* **D 71** (2005) 095008 [hep-ph/0412059].

[22] V. Berezinski et al.,*Searching for relic neutralinos using neutrino telescopes*, *Astropart. Phys.* **5** (1996) 333 [hep-ph/9603342];
P. Nath and R. Arnowitt, *Non-universal soft SUSY breaking and dark matter*, *Phys. Rev.* **D 56** (1997) 2820 [hep-ph/9701301];
A. Bottino, F. Donato, N. Fornengo and S. Scopel, *ComPatibility of the new DAMA/NaI data on an annual modulation effect in WIMP direct search with a relic neutralino in supergravity schemes*, *Phys. Rev.* **D 59** (1999) 095004 [hep-ph/9808459]; *Probing the supersymmetric parameter space by WIMP direct detection*, *Phys. Rev.* **D 63** (2001) 125003 [hep-ph/0010203];
J.R. Ellis, K.A. Olive and Y. Santoso, *The MSSM parameter space with non-universal Higgs masses*, *Phys. Lett.* **B 539** (2002) 107 [hep-ph/0204192];
J.R. Ellis, T. Falk, K.A. Olive and Y. Santoso, *Exploration of the MSSM with non-universal Higgs masses*, *Nucl. Phys.* **B 652** (2003) 259 [hep-ph/0210205];
M. Drees, *Supersymmetric dark matter 2004*, hep-ph/0410113;
H. Baer, A. Mustafayev, S. Profumo, A. Belyaev and X. Tata, *Direct, indirect and collider detection of neutralino dark matter in SUSY models with non-universal Higgs masses*, *JHEP* **07** (2005) 065 [hep-ph/0504001];
J. Ellis, S.F. King and J.P. Roberts, *The fine-tuning price of neutralino dark matter in models with non-universal Higgs masses*, arXiv:0711.2741.

[23] A. Birkedal-Hansen and B.D. Nelson, *The role of Wino content in neutralino dark matter*, *Phys. Rev.* **D 64** (2001) 015008 [hep-ph/0102075]; *Relic neutralino densities and detection rates with nonuniversal gaugino masses*, *Phys. Rev.* **D 67** (2003) 095006 [hep-ph/0211071];
H. Baer, A. Mustafayev, E.-K. Park and S. Profumo, *Mixed Wino dark matter: consequences for direct, indirect and collider detection*, *JHEP* **07** (2005) 046 [hep-ph/0505227].

[24] H. Baer et al., *Exploring the BWCA (Bino-Wino Co-Annihilation) scenario for neutralino dark matter*, *JHEP* **12** (2005) 011 [hep-ph/0511034].

[25] H. Baer, A. Mustafayev, E.-K. Park, S. Profumo and X. Tata, *Mixed higgsino dark matter from a reduced* SU(3) *gaugino mass: consequences for dark matter and collider searches*, *JHEP* **04** (2006) 041 [hep-ph/0603197].

[26] H. Baer, A. Mustafayev, H. Summy and X. Tata, *Mixed Higgsino dark matter from a large* SU(2) *gaugino mass*, *JHEP* **10** (2007) 088 [arXiv:0708.4003].

[27] M. Drees, *Phenomenological consequences of N = 1 supergravity theories with nonminimal kinetic energy terms for vector superfields*, *Phys. Lett.* **B 158** (1985) 409;
G. Anderson et al., *Report of the supersymmetry theory subgroup*, in *New directions in high energy physics*, proceedings of Snowmass 96, online at
http://www.slac.stanford.edu/pubs/snowmass96/PDF/SUP106.PDF;
G. Anderson, H. Baer, C.-h. Chen and X. Tata, *The reach of Fermilab Tevatron upgrades for* SU(5) *supergravity models with non-universal gaugino masses*, *Phys. Rev.* **D 61** (2000) 095005 [hep-ph/9903370].

[28] N. Arkani-Hamed, A. Delgado and G.F. Giudice, *The well-tempered neutralino*, *Nucl. Phys.* **B 741** (2006) 108 [hep-ph/0601041].

[29] F.E. Paige, S.D. Protopopescu, H. Baer and X. Tata, *ISAJET 7.69: a Monte Carlo event generator for pp, p̄p and e^+e^- reactions*, `hep-ph/0312045`;
see also H. Baer, J. Ferrandis, S. Kraml and W. Porod, *On the treatment of threshold effects in SUSY spectrum computations*, *Phys. Rev.* **D 73** (2006) 015010 [`hep-ph/0511123`].

[30] H. Baer, A. Mustafayev, E.-K. Park and X. Tata, *Target dark matter detection rates in models with a well-tempered neutralino*, *JCAP* **01** (2007) 017 [`hep-ph/0611387`].

[31] H. Baer and X. Tata, *Probing charginos and neutralinos beyond the reach of LEP at the Tevatron collider*, *Phys. Rev.* **D 47** (1993) 2739.

[32] H. Baer, K. Hagiwara and X. Tata, *Gauginos as a signal for supersymmetry at pp̄ colliders*, *Phys. Rev.* **D 35** (1987) 1598;
H. Baer, D.D. Karatas and X. Tata, *Gluino and squark production in association with gauginos at hadron supercolliders*, *Phys. Rev.* **D 42** (1990) 2259;
H. Baer, C. Kao and X. Tata, *Aspects of chargino-neutralino production at the Tevatron collider*, *Phys. Rev.* **D 48** (1993) 5175 [`hep-ph/9307347`];
H. Baer, C.-H. Chen, F. Paige and X. Tata, *Trileptons from chargino-neutralino production at the CERN Large Hadron Collider*, *Phys. Rev.* **D 50** (1994) 4508 [`hep-ph/9404212`];
I. Hinchliffe, F.E. Paige, M.D. Shapiro, J. Soderqvist and W. Yao, *Precision SUSY measurements at LHC*, *Phys. Rev.* **D 55** (1997) 5520 [`hep-ph/9610544`];
I. Hinchliffe and F.E. Paige, *Measurements in gauge mediated SUSY breaking models at LHC*, *Phys. Rev.* **D 60** (1999) 095002 [`hep-ph/9812233`];
H. Bachacou, I. Hinchliffe and F.E. Paige, *Measurements of masses in SUGRA models at LHC*, *Phys. Rev.* **D 62** (2000) 015009 [`hep-ph/9907518`];
ATLAS collaboration, *ATLAS detector and physics performance technical design report*, LHCC 99-14/15;
C.G. Lester, M.A. Parker and M.J. White, *Determining SUSY model parameters and masses at the LHC using cross-sections, kinematic edges and other observables*, *JHEP* **01** (2006) 080 [`hep-ph/0508143`].

[33] For the preliminary bounds on sparticle masses from the combined LEP2 searches for sparticles, see http://lepsusy.web.cern.ch/lepsusy/.

[34] ALEPH collaboration, S. Schael et al., *Search for neutral MSSM Higgs bosons at LEP*, *Eur. Phys. J.* **C 47** (2006) 547 [`hep-ex/0602042`].

[35] B.C. Allanach, A. Djouadi, J.L. Kneur, W. Porod and P. Slavich, *Precise determination of the neutral Higgs boson masses in the MSSM*, *JHEP* **09** (2004) 044 [`hep-ph/0406166`].

[36] H. Baer, T. Krupovnickas and X. Tata, *Reach of the Fermilab Tevatron for minimal supergravity in the region of large scalar masses*, *JHEP* **07** (2003) 020 [`hep-ph/0305325`].

[37] PARTICLE DATA GROUP collaboration, W.M. Yao et al., *Review of particle physics*, *J. Phys.* **G 33** (2006) 1;
for the recent results from the E821 collaboration, MUON G-2 collaboration, G.W. Bennett et al., *Final report of the muon E821 anomalous magnetic moment measurement at BNL*, *Phys. Rev.* **D 73** (2006) 072003 [`hep-ex/0602035`] and references cited therein.

[38] D. Auto, H. Baer, A. Belyaev and T. Krupovnickas, *Reconciling neutralino relic density with Yukawa unified supersymmetric models*, *JHEP* **10** (2004) 066 [`hep-ph/0407165`].

[39] B.C. Allanach, S.F. King and D.A.J. Rayner, *Phenomenology of twisted moduli in type-I string inspired models*, *JHEP* **05** (2004) 067 [`hep-ph/0403255`];

S.F. King and J.P. Roberts, *Natural implementation of neutralino dark matter*, *JHEP* **09** (2006) 036 [hep-ph/0603095].

[40] H. Baer, C.-H. Chen, F. Paige and X. Tata, *Detecting sleptons at hadron colliders and supercolliders*, *Phys. Rev.* **D 49** (1994) 3283 [hep-ph/9311248].

[41] J.L. Feng, A. Rajaraman and B.T. Smith, *Minimal supergravity with $m(0)^2 < 0$*, *Phys. Rev.* **D 74** (2006) 015013 [hep-ph/0512172].

[42] H. Baer, M. Bisset, X. Tata and J. Woodside, *Supercollider signals from gluino and squark decays to Higgs bosons*, *Phys. Rev.* **D 46** (1992) 303.

[43] H. Baer and J. O'Farrill, *Probing neutralino resonance annihilation via indirect detection of dark matter*, *JCAP* **04** (2004) 005 [hep-ph/0312350].

[44] T. Blazek, R. Dermisek and S. Raby, *Yukawa unification in* SO(10), *Phys. Rev.* **D 65** (2002) 115004 [hep-ph/0201081].

[45] G. Anderson, H. Baer, C.-H. Chen and X. Tata, *The reach of Fermilab Tevatron upgrades for* SU(5) *supergravity models with non-universal gaugino masses*, *Phys. Rev.* **D 61** (2000) 095005 [hep-ph/9903370].

[46] R. Dermisek and A. Mafi, SO(10) *grand unification in five dimensions: proton decay and the μ problem*, *Phys. Rev.* **D 65** (2002) 055002 [hep-ph/0108139].

[47] A. Brignole, L.E. Ibáñez and C. Muñoz, *Towards a theory of soft terms for the supersymmetric standard model*, *Nucl. Phys.* **B 422** (1994) 125 [hep-ph/9308271].

[48] K. Choi, K.S. Jeong and K.-I. Okumura, *Phenomenology of mixed modulus-anomaly mediation in fluxed string compactifications and brane models*, *JHEP* **09** (2005) 039 [hep-ph/0504037];
M. Endo, M. Yamaguchi and K. Yoshioka, *A bottom-up approach to moduli dynamics in heavy gravitino scenario: superpotential, soft terms and sparticle mass spectrum*, *Phys. Rev.* **D 72** (2005) 015004 [hep-ph/0504036];
A. Falkowski, O. Lebedev and Y. Mambrini, *SUSY phenomenology of KKLT flux compactifications*, *JHEP* **11** (2005) 034 [hep-ph/0507110];
H. Baer, E.-K. Park, X. Tata and T.T. Wang, *Collider and dark matter searches in models with mixed modulus-anomaly mediated SUSY breaking*, *JHEP* **08** (2006) 041 [hep-ph/0604253]; *Measuring modular weights in mirage unification models at the LHC and ILC*, *Phys. Lett.* **B 641** (2006) 447 [hep-ph/0607085]; *Collider and dark matter phenomenology of models with mirage unification*, *JHEP* **06** (2007) 033 [hep-ph/0703024];
K. Choi, K.Y. Lee, Y. Shimizu, Y.G. Kim and K.-I. Okumura, *Neutralino dark matter in mirage mediation*, *JCAP* **12** (2006) 017 [hep-ph/0609132].

[49] L. Randall and R. Sundrum, *Out of this world supersymmetry breaking*, *Nucl. Phys.* **B 557** (1999) 79 [hep-th/9810155];
G.F. Giudice, M.A. Luty, H. Murayama and R. Rattazzi, *Gaugino mass without singlets*, *JHEP* **12** (1998) 027 [hep-ph/9810442].

[50] R. Kitano and Y. Nomura, *Supersymmetry, naturalness and signatures at the LHC*, *Phys. Rev.* **D 73** (2006) 095004 [hep-ph/0602096].

[51] H. Baer and T. Krupovnickas, *Radiative neutralino decay in supersymmetric models*, *JHEP* **09** (2002) 038 [hep-ph/0208277].

[52] G. Belanger, F. Boudjema, A. Cottrant, A. Pukhov and A. Semenov, *WMAP constraints on SUGRA models with non-universal gaugino masses and prospects for direct detection*, *Nucl. Phys.* **B 706** (2005) 411 [hep-ph/0407218];
Y. Mambrini and E. Nezri, *Dark matter and colliders searches in the MSSM*, *Eur. Phys. J.* **C 50** (2007) 949 [hep-ph/0507263].

[53] S. Martin, *Compressed supersymmetry and natural neutralino dark matter from top squark-mediated annihilation to top quarks*, *Phys. Rev.* **D 75** (2007) 115005 [hep-ph/0703097].

[54] H. Baer, A. Box, E.K. Park and X. Tata, *Implications of compressed supersymmetry for collider and dark matter searches*, *JHEP* **08** (2007) 060;
S. Martin, *Top-squark-mediated annihilation scenario and direct detection of dark matter in compressed supersymmetry*, *Phys. Rev.* **D 76** (2007) 095005 [arXiv:0707.2812].

[55] H. Baer, A. Mustafayev, S. Profumo and X. Tata,*Probing supersymmetry beyond the reach of LEP2 at the Fermilab Tevatron: low $|M^3|$ dark matter models*, *Phys. Rev.* **D 75** (2007) 035004 [hep-ph/0610154].

[56] H. Baer, J. Woodside and X. Tata, *Phenomenology of gluino decays via loops and top-quark Yukawa coupling*, *Phys. Rev.* **D 42** (1990) 1568.

[57] J. Mizukoshi, P. Mercadante and X. Tata, *Using b-tagging to enhance the supersymmetry reach of the CERN Large Hadron Collider*, *Phys. Rev.* **D 72** (2005) 035009 [hep-ph/0506142];
S.P. Das, A. Datta, M. Guchait, M. Maity and S. Mukherjee, *Focus Point SUSY at the LHC revisited*, arXiv:0708.2048.

[58] XENON collaboration, J. Angle et al., *First results from the XENON10 dark matter experiment at the Gran Sasso national laboratory*, *Phys. Rev. Lett.* **100** (2008) 021203 [arXiv:0706.0039].

[59] H. Baer, C. Balázs, A. Belyaev, T. Krupovnickas and X. Tata, *Updated reach of CERN LHC and constraints from relic density, $b \to s\gamma$ and $a\mu$ in the mSUGRA mode*, *JHEP* **06** (2003) 054;
see also, S. Abdullin and F. Charles, *Search for SUSY in (leptons +) jets + $E_T^{\rm miss}$ final states*, *Nucl. Phys.* **B 547** (1999) 60 [hep-ph/9811402];
CMS collaboration, S. Abdullin et al., *Discovery potential for supersymmetry in CMS*, *J. Phys.* **G 28** (2002) 469 [hep-ph/9806366];
B. Allanach, J. Hetherington, A. Parker and B. Webber, *Naturalness reach of the Large Hadron Collider in minimal supergravity*, *JHEP* **08** (2000) 017.

[60] H. Baer, J. Sender and X. Tata, *Search for top squarks at the Fermilab Tevatron collider*, *Phys. Rev.* **D 50** (1994) 4517 [hep-ph/9404342];
J. Sender, *Techniques for the top squark search at the Fermilab Tevatron*, hep-ph/0010025;
R. Demina, J. Lykken and K. Matchev, *Top and bottom squark searches in run II of the Fermilab Tevatron*, *Phys. Rev.* **D 62** (2000) 035011 [hep-ph/9910275].

[61] HEAVY FLAVOR AVERAGING GROUP collaboration, E. Barberio et al., *Averages of b-hadron properties at the end of 2005*, hep-ex/0603003.

[62] M. Misiak et al., *Estimate of $BR(B \to X_s\gamma)$ at $O(\alpha_s^2)$*, *Phys. Rev. Lett.* **98** (2007) 022002 [hep-ph/0609232].

[63] M. Davier, *The hadronic contribution to $(g-2)$ of the muon*, *Nucl. Phys.* **169** *(Proc. Suppl.)* (2007) 288 [hep-ph/0701163];
see also, K. Hagiwara, A.D. Martin, D. Nomura and T. Teubner, *Improved predictions for g2 of the muon and $\alpha_{QED}(M_Z^2)$*, *Phys. Lett.* **B 649** (2007) 173 [hep-ph/0611102].

[64] H. Baer, C. Balazs, A. Belyaev and J. O'Farrill, *Direct detection of dark matter in supersymmetric models*, *JCAP* **09** (2003) 007.

[65] J.R. Ellis, K.A. Olive and C. Savage, *Hadronic Uncertainties in the Elastic Scattering of Supersymmetric Dark Matter*, arXiv:0801.3656;
J.R. Ellis, K.A. Olive, Y. Santoso and V.C. Spanos, *Update on the direct detection of supersymmetric dark matter*, *Phys. Rev.* **D 71** (2005) 095007 [hep-ph/0502001].

[66] SUPERCDMS collaboration, R.W. Schnee et al., *The SuperCDMS experiment*, astro-ph/0502435.

[67] M. Tripathi, *LUX: a large two-phase liquid Xenon detector for WIMP search*, talk at *SUSY'07 meeting*, Karlsruhe, Germany 25 Jul-1 Ago (2007).

[68] THE XENON collaboration, E. Aprile, *The XENON dark matter experiment*, astro-ph/0502279.

[69] J. Ellis, R. Ferstl and K. Olive, *Re-evaluation of the elastic scattering of supersymmetric dark matter*, *Phys. Lett.* **B 481** (2000) 304 [hep-ph/0001005].

[70] G. Bertone, D.G. Cerdeño, J.I. Collar and B.C. Odom, *WIMP identification through a combined measurement of axial and scalar couplings*, *Phys. Rev. Lett.* **99** (2007) 151301 [arXiv:0705.2502].

[71] H. Baer, A. Belyaev, T. Krupovnickas and J. O'Farrill, *Indirect, direct and collider detection of neutralino dark matter*, *JCAP* **08** (2004) 005 [hep-ph/0405210].

[72] V. Barger, W.-Y. Keung, G. Shaughnessy and A. Tregre, *High energy neutrinos from neutralino annihilations in the Sun*, *Phys. Rev.* **D 76** (2007) 095008 [arXiv:0708.1325].

[73] P. Gondolo et al., *DarkSUSY: computing supersymmetric dark matter properties numerically*, *JCAP* **07** (2004) 008 [astro-ph/0406204].

[74] THE ICECUBE collaboration, J. Ahrens et al., *IceCube: the next generation neutrino telescope at the South Pole*, *Nucl. Phys.* **118** *(Proc. Suppl.)* (2003) 388 [astro-ph/0209556];
F. Halzen, *High-energy neutrino astronomy: from AMANDA to IceCube*, astro-ph/0311004;
F. Halzen and D. Hooper, *IceCube-Plus: an ultra-high energy neutrino telescope*, *JCAP* **01** (2004) 002 [astro-ph/0310152].

[75] J.F. Navarro et al., *The inner structure of LambdaCDM Halos III: universality and asymptotic slopes*, *Mon. Not. Roy. Astron. Soc.* **349** (2004) 1039 [astro-ph/0311231];
the adiabatic contraction of the halo follows G.R. Blumenthal, S.M. Faber, R. Flores and J.R. Primack, *Contraction of dark matter galactic halos due to baryonic infall*, *Astrophys. J.* **301** (1986) 27.

[76] A. Burkert, *The structure of dark matter haloes in dwarf galaxies*, *Astrophys. J.* **447** (1995) L25 [astro-ph/9504041];
P. Salucci and A. Burkert, *Dark matters scaling relations*, *Astrophys. J.* **537** (2000) L9.

[77] GLAST collaboration, A. Morselli, A. Lionetto, A. Cesarini, F. Fucito and P. Ullio, *Search for dark matter with GLAST*, *Nucl. Phys.* **113** *(Proc. Suppl.)* (2002) 213 [astro-ph/0211327].

[78] S. Profumo and P. Ullio, *The role of antimatter searches in the hunt for supersymmetric dark matter*, *JCAP* **07** (2004) 006 [hep-ph/0406018].

[79] S. Profumo and C.E. Yaguna, *A statistical analysis of supersymmetric dark matter in the MSSM after WMAP*, *Phys. Rev.* **D 70** (2004) 095004 [hep-ph/0407036].

[80] K. Mori et al., *A novel antimatter detector based on X-ray deexcitation of exotic atoms*, *Astrophys. J.* **566** (2002) 604 [astro-ph/0109463];
C.J. Hailey et al., *Accelerator testing of the General Antiparticle Spectrometer, a novel approach to indirect dark matter detection*, *JCAP* **01** (2006) 007 [astro-ph/0509587].

[81] H. Baer and S. Profumo, *Low energy antideuterons: shedding light on dark matter*, *JCAP* **12** (2005) 008 [astro-ph/0510722].

[82] PAMELA collaboration, M. Pearce, *The status of the PAMELA experiment*, *Nucl. Phys.* **113** *(Proc. Suppl.)* (2002) 314.

[83] A.M. Green, *Determining the WIMP mass using direct detection experiments*, *JCAP* **08** (2007) 022 [hep-ph/0703217];
C.-L. Shan and M. Drees, *Determining the WIMP mass from direct dark matter detection data*, arXiv:0710.4296.

[84] E.A. Baltz, M. Battaglia, M.E. Peskin and T. Wizansky, *Determination of dark matter properties at high-energy colliders*, *Phys. Rev.* **D 74** (2006) 103521 [hep-ph/0602187].

[85] S.F. King, J.P. Roberts and D.P. Roy, *Natural dark matter in SUSY GUTs with non-universal gaugino masses*, *JHEP* **10** (2007) 106;
S.F. King and J.P. Roberts, *Natural dark matter from type I string theory*, *JHEP* **01** (2007) 024.